NACA RM L58A27

NACA

RESEARCH MEMORANDUM

JET EFFECTS ON THE BASE DRAG OF A CYLINDRICAL AFTERBODY WITH EXTENDED NOZZLES

By William J. Nelson and William R. Scott

Langley Aeronautical Laboratory
Langley Field, Va.

NATIONAL ADVISORY COMMITTEE
FOR AERONAUTICS

WASHINGTON
April 15, 1958
Declassified October 28, 1960

NACA RM L58A27

NATIONAL ADVISORY COMMITTEE FOR AERONAUTICS

RESEARCH MEMORANDUM

JET EFFECTS ON THE BASE DRAG OF A CYLINDRICAL AFTERBODY WITH EXTENDED NOZZLES

By William J. Nelson and William R. Scott

SUMMARY

A wind-tunnel investigation of the effects of both single and twin jets on base drag has been conducted at Mach numbers from 0.6 to 1.4. The plane of the jet exit was varied from that of the afterbody base to approximately one body diameter downstream. Several base ventilation systems were tested in conjunction with the twin-jet configurations. Significant improvements in base drag were obtained when the plane of the jet was extended as little as one-third of the body diameter beyond the base; the gains were less than those obtained with near optimum boattailing but significantly greater than with a boattail angle of 30°. Venting the base cavity to the external stream also reduced base drag; the extent of the improvement, however, varied considerably with method of venting; perforations were more effective than slots parallel to the axis, and strong gains were effected by scooping air from the boundary layer.

INTRODUCTION

The force produced by low pressures acting on the base of a bluff body housing a jet engine often represents a major drag component on transonic airplanes and missiles. These low pressures find their origin in the mixing along both the wake and jet boundaries. Many experimental investigations have been conducted to determine the relative magnitude of the stream and jet effects on base pressure and on the flow over boattailed bodies. (For example, see refs. 1 to 4.)

The present investigation was initiated to determine the feasibility of reducing the jet effect by extending the nozzle beyond the base of the afterbody. Thus, it was reasoned, the jet mixing zone would not influence the pressures in the dead air region adjacent to the base. In order to check this line of reasoning, two models of widely different configurations were designed and tested. The first model was

representative of single engine designs in which the propulsive jet is discharged from a sonic nozzle whose axis coincides with the axis of the afterbody. The second model was a two-jet configuration in which twin supersonic nozzles were mounted in the base of a cylindrical body with their axes parallel to that of the body. With the latter configuration attempts were also made to increase base pressure by venting the base cavity to the external stream in an effort to realize the favorable effects of base bleed reported by several experimenters. (For example, see ref. 5.) Several types of vents were tested including axial and circumferential slots, perforations, and auxiliary scoops to bring air into the base cavity.

The investigation reported herein is part of a general study of the effects of single and multiple jets on the drag of various afterbody configurations in the transonic regime. Wind-tunnel tests cover the Mach number range from 0.60 to 1.40; the corresponding Reynolds number range was 3.3×10^6 to 4.4×10^6 per foot. Sonic nozzles were operated at jet total-pressure ratios up to 5; and supersonic (Mach number 2.5) nozzles up to 20. The boundary layer approaching the base was turbulent. The test conditions simulate the zero-angle-of-attack case only.

SYMBOLS

The following symbols are used in this report:

A	area
C_D	drag coefficient, $-C_{p,b}\left(1 - \frac{A_j}{A_m}\right)$
C_p	pressure coefficient, $\frac{p - p_o}{q_o}$
d	diameter
H	total pressure
l	length of nozzle relative to base (positive when nozzle extends downstream of base)
M	Mach number
p	static pressure

q	dynamic pressure
r	radius
β	boattail angle

Subscripts:

b	base
c	plenum chamber
d	design
e	nozzle exit
j	jet
m	maximum
n	nozzle
o	free stream

APPARATUS

The $4\frac{1}{2}$ by $4\frac{1}{2}$-inch slotted test section used in this investigation is shown in the photograph of figure 1(a) and in the sketch of figure 1(b). The top and bottom walls of the test section contained four slots each, the width of the slots was such that the ratio of the open area to the total area of the slotted walls was 1:8. Construction details of this tunnel and the Mach number distribution along the empty test section are presented in reference 6. Air enters the test section at a maximum stagnation pressure of two atmospheres and is returned to the atmosphere through a diffuser (area ratio 1.75:1). Suction was applied to the chamber surrounding the test section through auxiliary pumps to reduce the test-section pressure and thus provide Mach number control over the range above 1.0. In the subsonic range the Mach number was controlled by varying the stream stagnation pressure. The stagnation pressure of the stream was measured in the upstream 30-inch supply duct; the test-section reference static pressure p_c was measured in the tunnel plenum chamber. The stream stagnation temperature was elevated to a maximum of 250° F to avoid condensation.

The models were attached to a 1-inch-diameter sting supported along the center line of the tunnel as shown in figure 1(b). This sting was also used as a supply tube for the air which was ducted to the jet nozzles. This air was stored in outside tanks at approximately 250 pounds per square inch and at atmospheric temperature.

The models studied in this investigation are shown in figures 2 and 3. The diameter of the sonic nozzle (fig. 2) was equal to 62.5 percent of the base diameter. The base static pressure was measured at a point approximately 0.08 inch from the rim; the jet total pressure was measured in the supply pipe; and both were recorded continuously. Data figure numbers corresponding to specific configurations are also indicated in this figure.

The basic twin-nozzle ($M_n = 2.5$) configurations tested are indicated in figure 3(a) where the coordinates are also given. The diameter of each of these nozzles was equal to 32.5 percent of the base diameter and they were separated 1.2 jet diameters at the center lines. Again data figure numbers corresponding to the various configurations tested are presented. Photographs of several skirt configurations tested are shown in figure 3(b). The skirt configurations were of four basic lengths; two configurations had six equally spaced longitudinal slots with the open area to total area ratios of 1:4 to 1:2; one had a circumferential slot (0.032 inch deep) inclined at 8° to the axis; and one was perforated with an open area to total area ratio of approximately 1:3. The perforated skirt was also tested with scoops over the upstream row of holes to increase the flow of air into the base cavity. The scoops on this model extended 0.120 inch into the external stream and they had a total open area of 0.07 square inch. With all these models, the base pressure was simultaneously recorded at two points as indicated in figure 3(a). As in tests of the single jet models, the base pressures were fed into transducers and recorded on pen-trace potentiometers.

RESULTS AND DISCUSSION

For convenience in presentation and discussion, the results of this investigation are divided into two sections. Both sections are concerned with the variations in base drag which accompany changes in stream Mach number and jet pressure ratio. Data presented in the first section were taken in tests with a single jet discharging from a sonic nozzle whose length was variable. In the second section, data obtained in tests with the twin supersonic jets discharging into the wake of the cylindrical body are presented; again the distance between the base of the afterbody and the exit plane of the nozzles was varied. In all tests the boundary layer approaching the base of the cylindrical afterbody was fully turbulent; its total thickness was about 20 percent of the body diameter; complete velocity distributions are presented in reference 7.

Single Nozzle - Sonic

Basic configuration.- With a propulsive jet discharging from a sonic nozzle whose exit was in the plane of the base, the base drag coefficient, at constant Mach number, varied with jet pressure ratio as shown in figure 4(a). As noted in many earlier investigations the jet, within the pressure ratio range of these tests, generally exerts an unfavorable influence on the drag of a cylindrical afterbody. The magnitude of the effect shown here is generally smaller than that reported in other investigations. Although these differences, which are attributed to differences in tunnel blockage, interference effects, model boundary layer, and so forth, affect comparisons with data from other sources, comparisons of these data within themselves are unaffected.

Effect of nozzle extension.- With the jet nozzle extended approximately one-third of the body diameter beyond the base, the variation in base drag resulting from increasing the jet pressure ratio was much smaller (fig. 4(b)) than with the flush nozzle. Comparison of these curves with those of the preceding figure shows that, for jet-pressure ratios greater than 2, the base drag coefficient was reduced about 40 percent by this short extension of the nozzle. Another 15 to 20 percent reduction in drag was obtained by doubling the nozzle length to two-thirds of the base diameter. (See fig. 4(c).) At this point jet-pressure ratio had very little effect on flow at the base; it is therefore not surprising that further extension of the nozzle had only a minor effect on base drag. (See fig. 4(d).) With larger jets (relative to the base) similar gains would be expected to accompany shorter nozzle extensions, and conversely, longer extensions would be required with smaller jets.

Although data are not available for direct comparison of the relative advantages of extended nozzle configurations and boattailed afterbodies, it is possible by comparing the drag of each with that of cylindrical bodies tested under the same conditions to determine their relative advantages. The reference configuration selected for this comparison is the cylindrical body with the jet exit in the base plane. Thus the drag increment between extended and flush nozzle configurations of the current study and between the boattailed and cylindrical configurations of reference 2 are compared in figure 5. The top group of 4 bars indicates a reduction in C_D of 0.085 from a one-third-diameter extension of the nozzle; for an 8° conical afterbody of equal length, a reduction in total afterbody drag of approximately 0.140 is indicated. Smaller gains are indicated at $\beta = 16^\circ$ and 30°, the latter being somewhat inferior to the extended nozzle. Extending the nozzle to five-eights of the base diameter resulted in a 0.135 gain in drag coefficient which was again exceeded by both 8° and 16° bodies, the drag of the 30° body is not shown since its length would have been substantially less than that of

the extended nozzle. Similarly, at $l/d = 0.96$ the drag reduction realized by extending the nozzle was approximately 75 percent of that obtainable with the near optimum 8° conical afterbody. At lower pressure ratios the advantages of the boattail are generally smaller and increase at higher pressure ratios.

A cursory comparison of available data at $M = 1.2$ indicates that at this speed a slightly smaller proportion of the drag reduction attainable with a conical afterbody may be obtained by extension of the nozzle.

It has been shown that the adverse effect of the jet on the drag of a cylindrical body may be virtually eliminated by adequate extension of the nozzle. Although the nozzle extension effected substantial reductions in body drag, these configurations were inferior to the better boattailed afterbodies of equal length. The results, however, give rise to a suggestion that the extended nozzle be combined with the boattailed afterbody to effect further improvement in the latter. Although specific tests have not been made to establish the possible benefits of such a combination, the literature does contain data which are indicative of significant gains. In reference 8, Cahn has shown substantially lower afterbody drag when the jet was replaced with a solid sting whose shape was calculated to match the external shape of the jet. Since the present tests indicate that, with the nozzle extended two-thirds of the base diameter or more, the jet had relatively little effect on drag, it is concluded that Cahn's results would be approximated if the sting were replaced with a nozzle which was extended some two-thirds of the base diameter. It is probable that this gain would be realized with much shorter extensions since the nozzle diameter relative to base diameter would be much larger with the boattailed body. A similar conclusion is drawn from flight data presented in reference 9 where the addition of a dummy sting to a boattailed afterbody ($\beta = 18\frac{1}{2}^{\circ}$) resulted in substantial increases in the base pressure coefficient at Mach numbers from 0.6 to 1.8.

Twin Nozzles - Supersonic

Effect of nozzle extension.- The twin-jet configuration with $M_n = 2.5$ nozzles is representative of rocket-powered missile designs. Because significant differences in pressure were sometimes measured at the two base orifice locations, the data are presented in terms of the base pressure coefficient rather than base drag. In figure 6, $C_{p,b}$ is plotted as a function of the jet pressure ratio for several Mach numbers from 0.6 to 1.4. For those configurations in which the afterbody skirt is extended to or beyond the exit plane of the nozzles, the base pressure of both measuring points was the same and therefore only one curve appears at each Mach number in figures 6(a) and 6(b). For

configurations in which the nozzles were extended beyond the skirt, the solid line (fig. 6(d)) indicates data obtained at the outboard measuring point and the dotted line, that obtained near the model axis. At subsonic speeds the variation in $C_{p,b}$ for even the high drag configurations was largely restricted to $H_j/p_o = 6$ or less. Supersonically, the base pressure decreased steadily throughout the operating range of this program. As in the single jet tests, extending the nozzles downstream significantly reduced the adverse jet effects. At the design pressure ratio of the nozzle (17.1), the minimum base pressure coefficient recorded with the longest nozzle extension was -0.28 and occurred at $M = 1.10$. (See fig. 6(d).) With the skirt terminated in plane of nozzle exit, the minimum value of $C_{p,b}$ was approximately -0.4 (fig. 6(b)) and, with the skirt overhanging the nozzle, approached -0.5 (fig. 6(a)).

Schlieren photographs of the flow over these models at several Mach numbers and jet pressure ratios are presented in figure 7. The individual pictures are arranged in order of increasing Mach number from left to right and in order of increasing jet pressure from top to bottom. Numerals in the lower right corner of each picture indicate the approximate jet pressure ratio; variations in H_j/p_o across the figure result from the fact that, although the jet pressure was held constant, the tunnel static pressure decreased with increasing Mach number.

For the extended skirt configurations (figs. 7(a) and 7(b)), the wake boundary is clearly defined for the jet-off condition but for the jet-on condition becomes confused with the jet boundary at a point very close to the base of the model. The wake convergence leads to expansion of the external flow close to the model followed by a region of compression as the streamlines again turn parallel to the body axis. At subsonic Mach numbers the pressure gradients through these regions are small and not easily detected by the schlieren system; at supersonic speeds, however, they are clearly defined. The initial wake convergence angle is determined by the base pressure and therefore increases with jet pressure ratio. Turning of the external flow as it intersects the jet boundary leads to the distributed compressions which develop into finite shock waves at a short distance from the axis of the body. Increased steepness of these shock waves with increasing jet pressure ratio results from the combination of greater initial turning of the external flow and increased divergence of the jet boundary. At the highest pressure ratio and maximum Mach number, a second shock wave appears; this wave has its origin in the overexpanded jet and is propagated outward through the supersonic mixing zone as a discrete wave. The presence of this shock wave within the jet is characteristic of off-design operation; its absence from the external flow at other

operating conditions indicates that the mixing zone was subsonic at the point where the shock reached the jet boundary.

Extending the jet nozzles effects an overall weakening of the shock waves but only minor changes in the general flow pattern. (See fig. 7(c).) The greatest difference occurs in the jet-off condition where the converging wake impinges on the nozzles themselves to set up a pattern very much like that observed earlier in the jet-on tests.

Effect of base ventilation.- Previous investigations (ref. 5, for example) have shown that large improvements in base pressure can often be obtained by bleeding very small quantities of air into the wake at the base of a bluff body. In the present program several attempts were made to increase base pressure by opening passages through the afterbody to permit air from the external stream to bleed into the base cavity. Nozzle extensions of 0.020 and -0.210 inch were selected for these tests, the results of which are presented in figure 8.

Venting the base through six longitudinal slots resulted in only minor changes in base pressure at the lower Mach numbers but at the higher speeds the variation in $C_{p,b}$ with jet pressure ratio was virtually eliminated. With the slots oriented so that two were in the plane of symmetry through the orifices, the two base pressures were separated by a small amount as indicated in figures 8(a) and 8(b) by the solid and dotted lines. It is possible that this difference is influenced by the slot orientation relative to the nozzles and orifices. Near the design pressure ratio (17.1) longitudinal slotting of the skirt had a favorable effect on the base pressure, the greatest improvement occurring at the higher speeds. Below the design point, however, the effectiveness of the slots in elevating base pressure falls rapidly at the supersonic speeds and more slowly at the lower Mach numbers; this results in significant losses in performance at the lower pressure ratios. For these configurations the effect of skirt length was unaltered by the slotting; for example, the longer skirts resulted in lower base pressures and consequently in higher drag. Substantial gains relative to the no bleed configuration were realized when the slots were widened to provide an open area equal to 52 percent of the perimeter. (See fig. 8(c).)

With three transverse slots inclined at 8° to the external stream, the base pressure (figs. 8(d) and 8(e)) followed closely the pattern of the unslotted configurations. Data taken at two measuring stations on the base were identical and are therefore represented at each Mach number by a single line. The base pressure coefficient was generally smaller at supersonic speeds and slightly larger at $M < 1$ than in the unslotted configurations. Adding the induction drag of the slot as an

air inlet results in even larger adverse effects at low Mach numbers and in the reduction of possible gains at the higher speeds.

Perforations of the skirt offered still another means of venting the low pressure region at the base to the ambient pressure along the body ahead of the base. Tests of the shorter afterbodies with a perforated rather than slotted skirt resulted in the pressures shown in figure 8(f). Here also the effect of the jet was small, the base pressures remaining essentially constant over the entire range of this investigation. Separation of the two base pressures was somewhat greater than with the slotted configurations; however, the level of the base pressure was higher than with the previously discussed configurations, and hence, the base drag would be smaller.

Figure 8(g) shows data obtained when small scoops were added to the front row of perforations. Again the jet-pressure ratio had a relatively small effect but the level of the pressure was significantly higher than with the flush slots and perforations. Because no attempt was made to refine the external fairing of the scoops, local velocities at the end of the skirt may have been significantly different from those for the unmodified configurations.

The results of tests with vented base models are summarized on figure 9 where the mean base pressure at the design pressure ratio $\left(H_j/p_o = 17.1\right)$ is plotted as a function of stream Mach number. Only the data from tests with the skirt terminated in the plane of the exit nozzles, $l/d = 0.020$, are presented since they are more complete. Minor extrapolations of the data were necessary where the tests were terminated below the design pressure ratio. The slotted configurations, as previously indicated, provide relatively small gains when the slot area was 26 percent of the total skirt area but, when increased to 52 percent, was substantially superior to the basic configuration. The perforated configuration is shown to be substantially superior to the unventilated configuration and the addition of scoop inlets to the forward row of holes reduced the negative value of $C_{p,b}$ further. With scoops the improvement in base pressure coefficient corresponds to approximately a 60- to 70-percent reduction in drag at $M = 1.3$. Base pressure, of course, is only part of the story for it gives no indication of the drag associated with the induction of the bleed air. Since the longitudinal slots were open at the back, it seems unlikely that any great drag force would have been associated with them whereas, for the perforated and transversely slotted configuration and the scoops, high pressures on the forward facing surface might be expected to contribute rather substantial drag. Apparent advantages of these configurations over the longitudinally slotted configurations would therefore be reduced.

The schlieren photographs of figure 10 provide a qualitative idea of the external drag associated with the slotted and perforated configurations. Very weak shock waves which appear in figure 10(a) indicate that the external drag of the longitudinally slotted skirt was relatively small. With transverse slots (figs. 10(b) and 10(c)) however, a strong oblique shock originating at the inlet lips suggests appreciable pressure drag. Flow over the perforated skirt (fig. 10(d)) was characterized by numerous shock waves whose individual strength appears to be small; their cumulative drag, however, may be significant. Figure 10(e) shows numerous strong waves ahead of the scoop inlets followed by expansion and further shock waves over the fairings. Much of the drag associated with these shock waves could undoubtedly be eliminated by more attention to detail scoop design.

CONCLUSIONS

From the transonic tunnel tests of both single and twin-jet configurations with extended nozzles, it is concluded that:

1. The adverse jet effects on base drag can be sharply reduced by small extensions of the jet nozzle beyond the plane of the base.

2. The drag reductions effected, at Mach number of 0.9 and a jet total pressure ratio of 4, by extending the sonic nozzle beyond the base of a cylindrical body are less than those attainable by the addition of a near optimum boattail but greater than those obtained with a boattail angle of 30°.

3. Venting the base cavity to the ambient stream through longitudinal slotting of the afterbody skirt can effect significant improvements in base drag only if the slot area is relatively large (on the order of 50 percent of the skirt area); perforations with the hole axis inclined into the direction of flight are more effective than slots of equal area in reducing base drag. Base-drag reductions greater than those attainable with the extended nozzles can be obtained if the vent air is scooped from the external stream but the induction drag of such an installation may be high.

Langley Aeronautical Laboratory,
National Advisory Committee for Aeronautics,
Langley Field, Va., January 9, 1958.

REFERENCES

1. Cubbage, James M., Jr.: Jet Effects on Base and Afterbody Pressures of a Cylindrical Afterbody at Transonic Speeds. NACA RM L56C21, 1956.

2. Cubbage, James M., Jr.: Jet Effects on the Drag of Conical Afterbodies for Mach Numbers of 0.6 to 1.28. NACA RM L57B21, 1957.

3. Salmi, Reino J., and Klann, John L.: Investigation of Boattail and Base Pressures of Twin-Jet Afterbodies at Mach Number 1.91. NACA RM E55C01, 1955.

4. Leiss, Abraham: Free-Flight Investigation of Effects of Simulated Sonic Turbojet Exhaust on the Drag of Twin-Jet Boattail Bodies at Transonic Speeds. NACA RM L56D30, 1956.

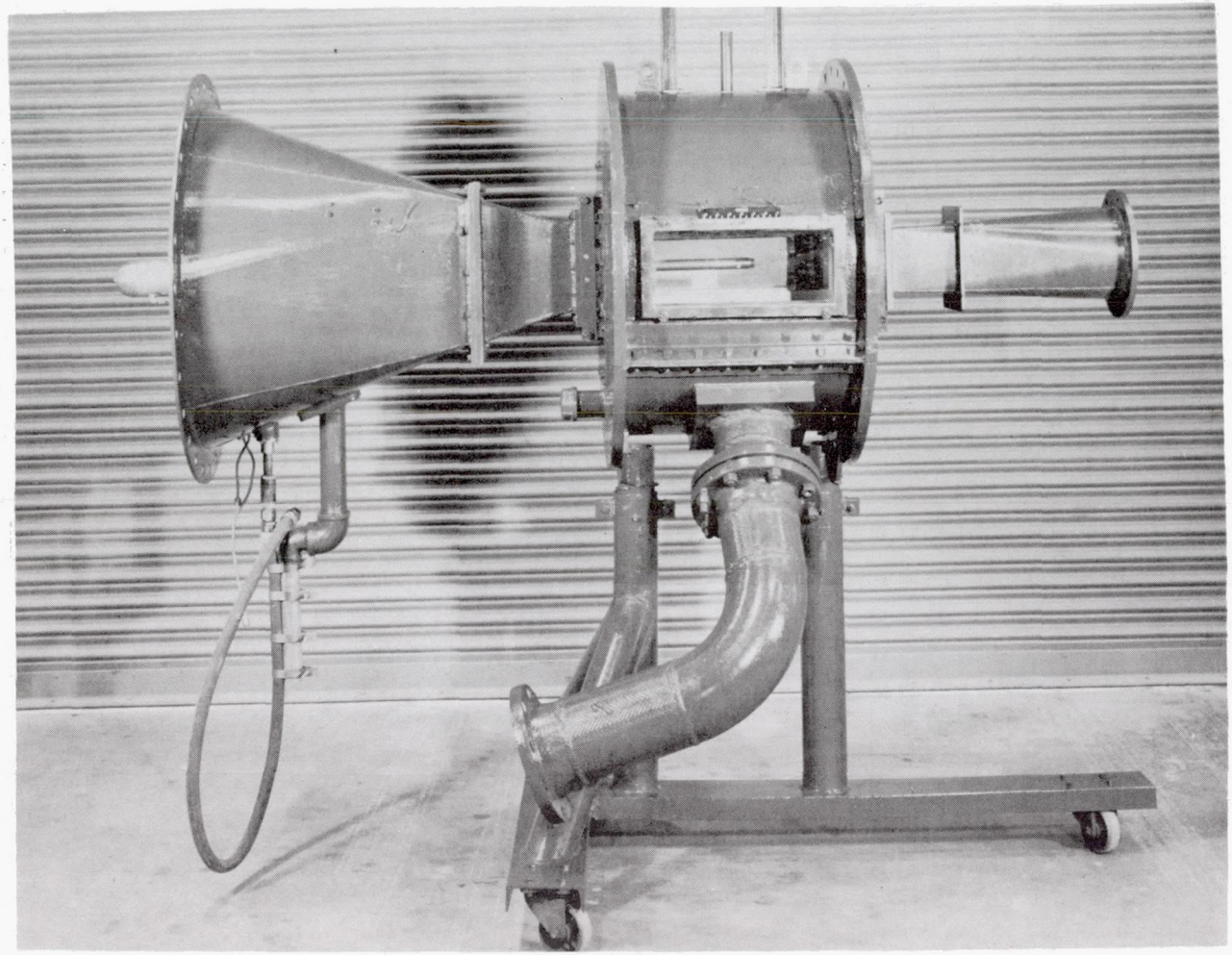
5. Cortright, Edgar M., Jr., and Schroeder, Albert H.: Preliminary Investigation of Effectiveness of Base Bleed in Reducing Drag of Blunt-Base Bodies in Supersonic Stream. NACA RM E51A26, 1951.

6. Nelson, William J., and Cubbage, James M., Jr.: Effects of Slot Location and Geometry on the Flow in a Square Tunnel at Transonic Mach Numbers. NACA RM L53J09, 1953.

7. Silhan, Frank V., and Cubbage, James M., Jr.: Drag of Conical and Circular-Arc Boattail Afterbodies at Mach Numbers From 0.6 to 1.3. NACA RM L56K22, 1957.

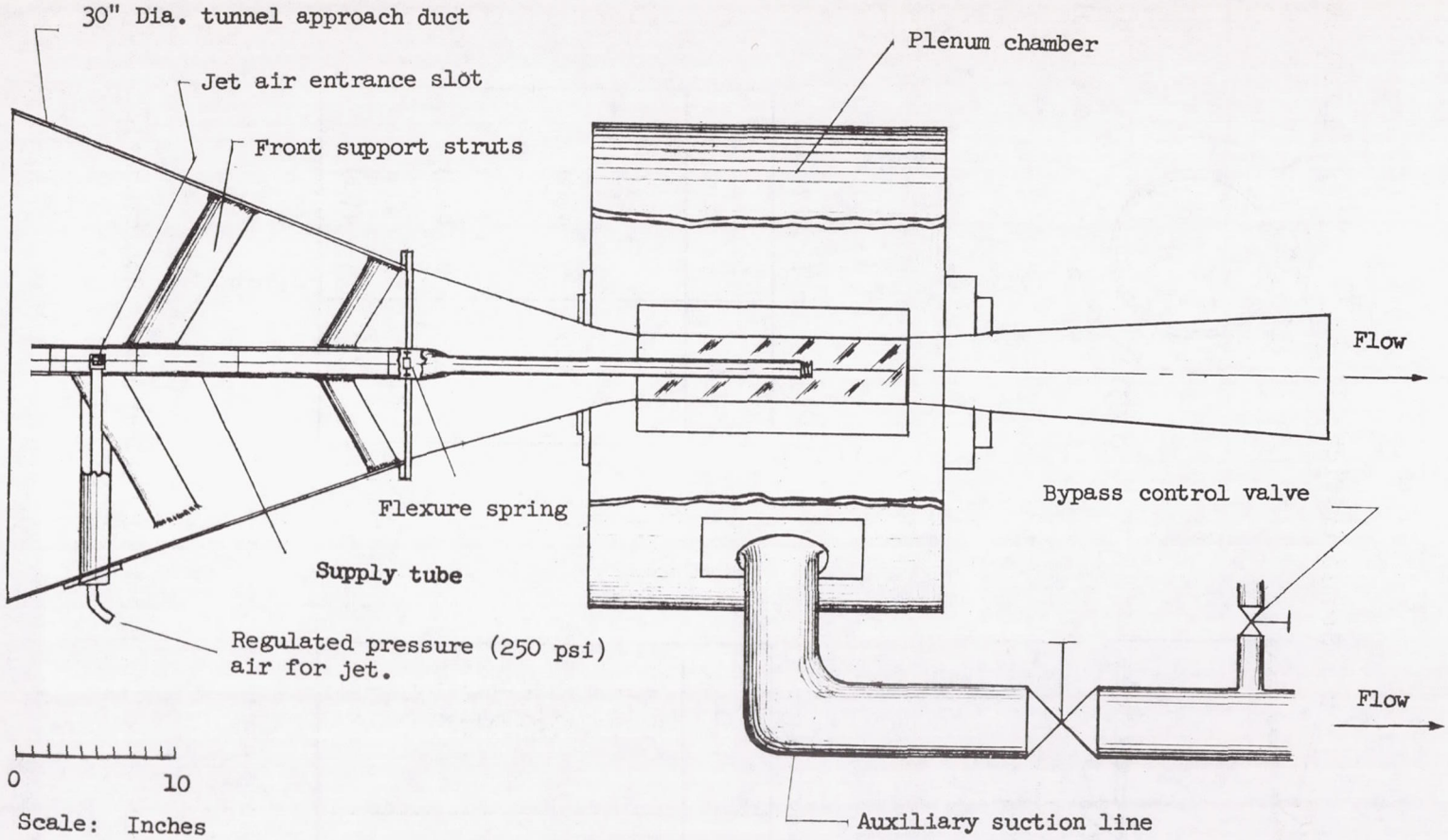
8. Cahn, Maurice S.: An Experimental Investigation of Sting-Support Effects on Drag and a Comparison With Jet Effects at Transonic Speeds. NACA RM L56F18a, 1956.

9. Stoney, William E., Jr.: Pressure Distributions at Mach Numbers From 0.6 to 1.9 Measured in Free Flight on a Parabolic Body of Revolution With Sharply Convergent Afterbody. NACA RM L51L03, 1952.



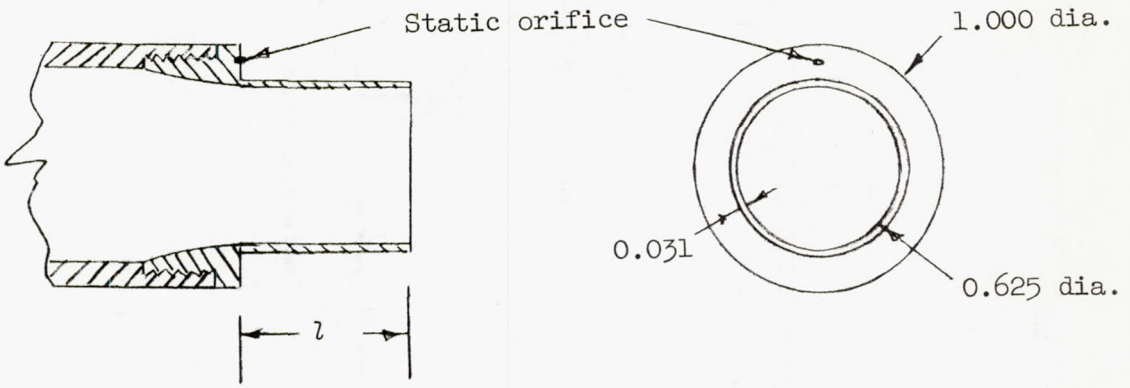
(a) $4\frac{1}{2}$ by $4\frac{1}{2}$ inch slotted test section. L-57-1178

Figure 1.- Tunnel and sting support.



(b) Sketch of tunnel showing ducting for jet flow.

Figure 1.- Concluded.



Nozzle coordinates

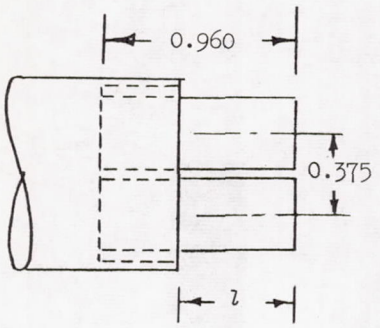
x,* in.	r, in.
0	0.314
.138	.314
.188	.314
.238	.323
.288	.332
.338	.341
.388	.350
.438	.359
.488	.368
.538	.377
.563	.382

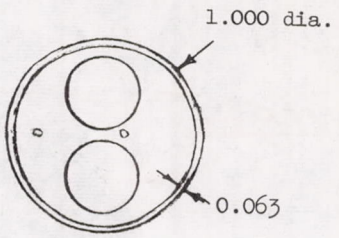
*Distance ahead of base plane

Test configurations

l	Data given in figure
0	4(a)
.315	4(b)
.625	4(c)
.958	4(d)

Figure 2.- Single jet configurations. Sonic nozzle.





o Static orifices

Supersonic nozzle coordinates

x,* in.	r, in.
0	0.100
.080	.113
.095	.115
.115	.117
.133	.121
.205	.132
.257	.138
.305	.144
.364	.150
.449	.156
.513	.159
.568	.161
.626	.162
.716	.163
.785	.163

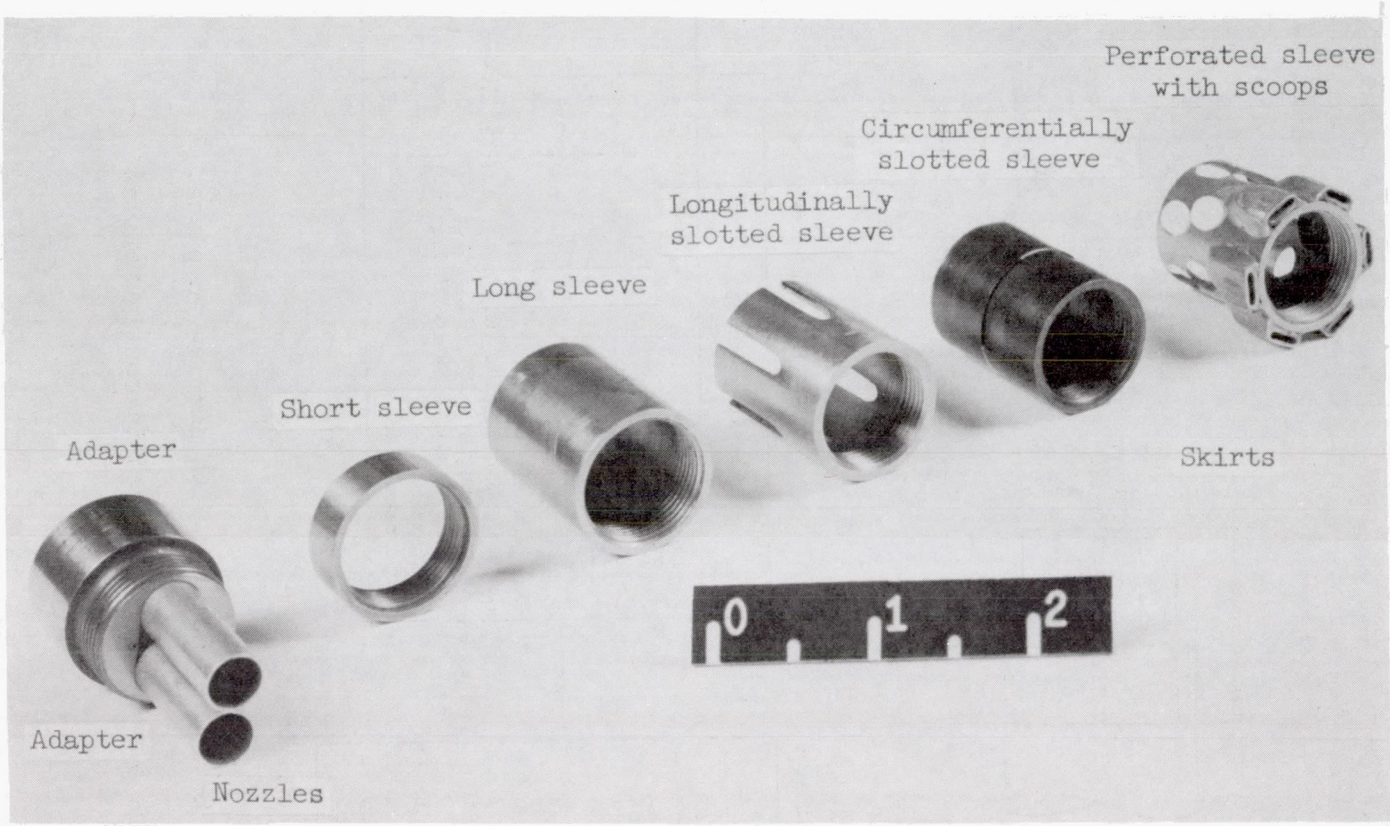
*Distance back of sonic throat

Test configurations

Sleeve geometry	l	Data presented in figure
Solid	-0.21	6(a)
Solid	.02	6(b)
Solid	.48	6(c)
Solid	.96	6(d)
Longitudinal slots (1/4 open)	-.21	8(a)
Longitudinal slots (1/4 open)	.02	8(b)
Longitudinal slots (1/2 open)	.02	8(c)
Circumferential slot (0.076 sq in.)	-.21	8(d)
Circumferential slot (0.076 sq in.)	.02	8(e)
Circumferential slot (0.076 sq in.)	.02	8(f)
Perforated	.02	8(f)
Perforated + scoops	.02	8(g)

(a) Sketch of adapter with nozzles in place.

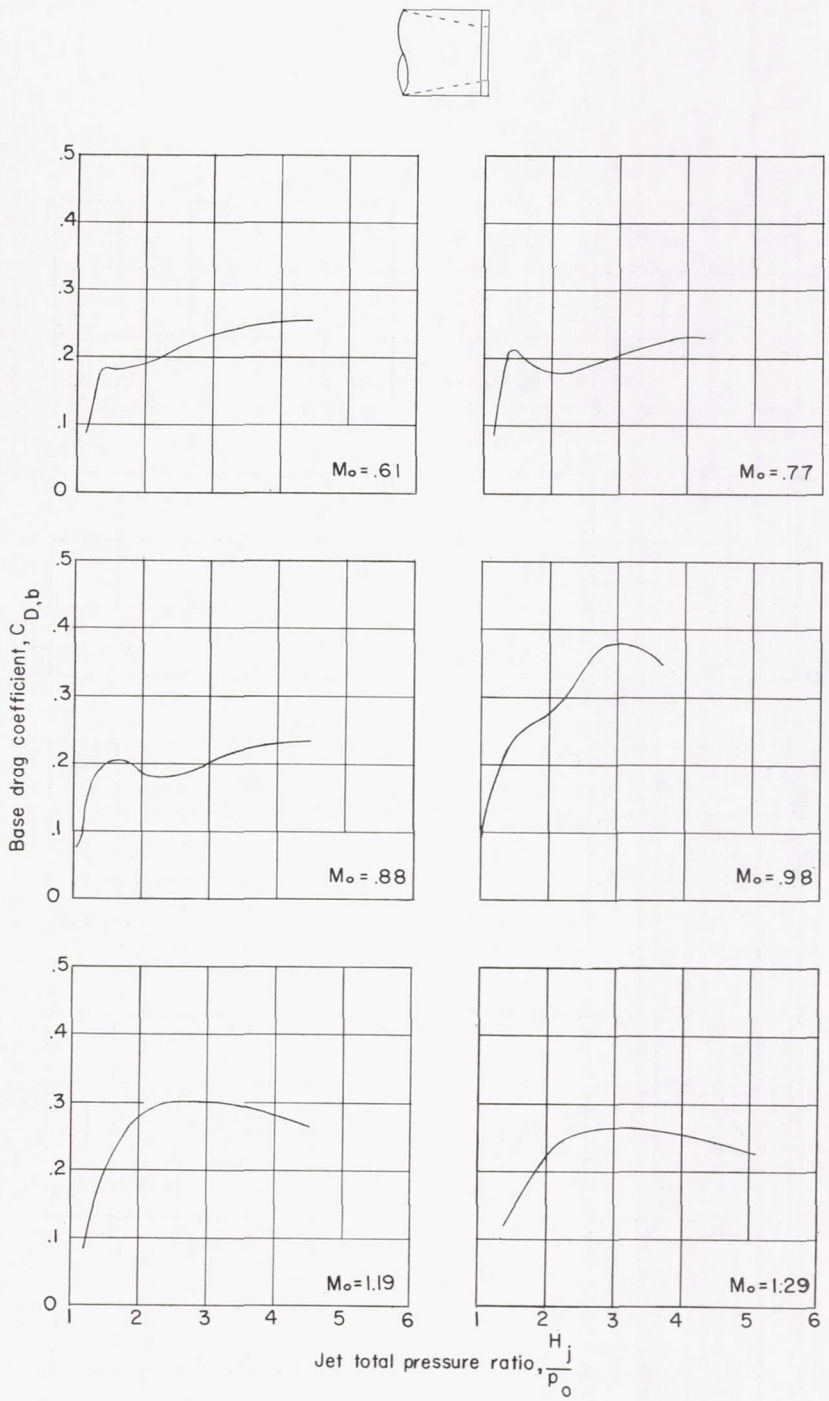
Figure 3.- Twin-jet supersonic configurations.



L-57-1181.1

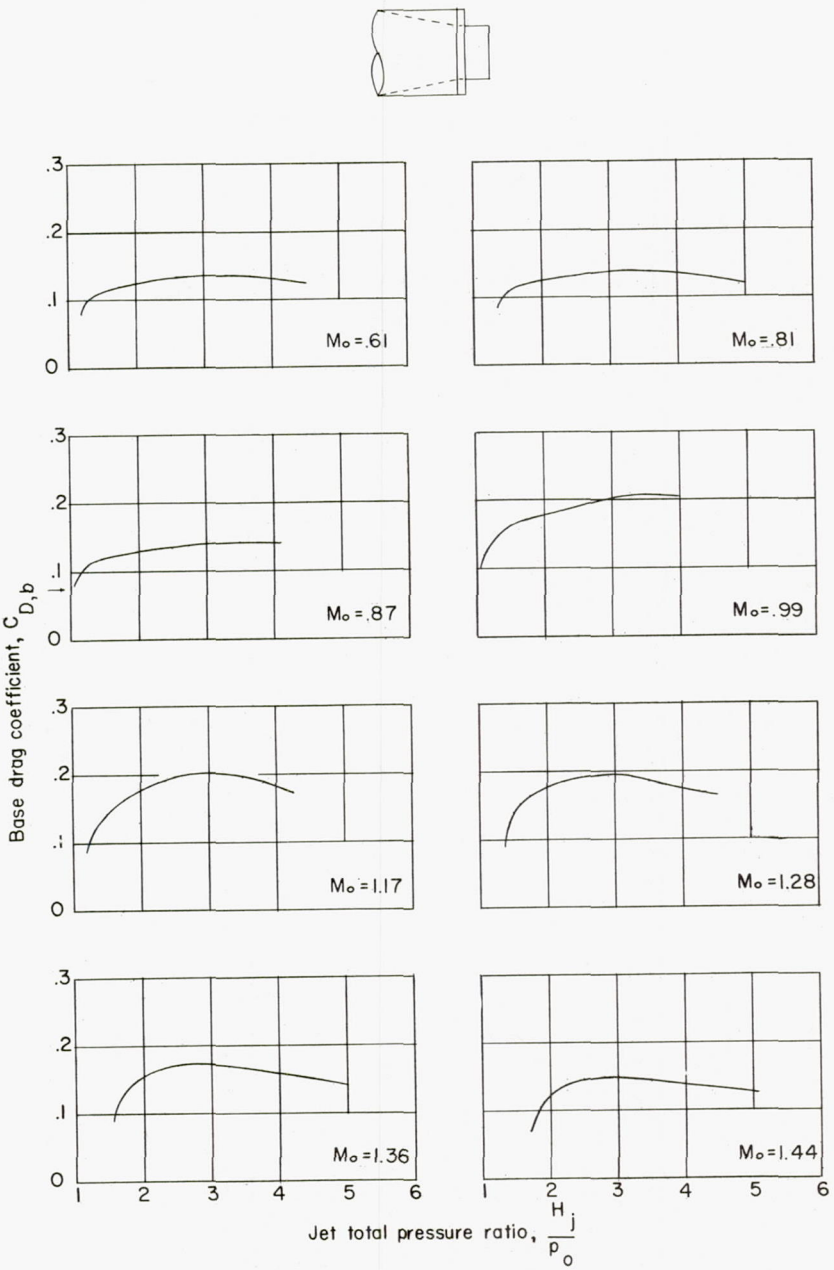
(b) Photograph of several skirts and adapter with supersonic nozzles in place.

Figure 3.- Concluded.



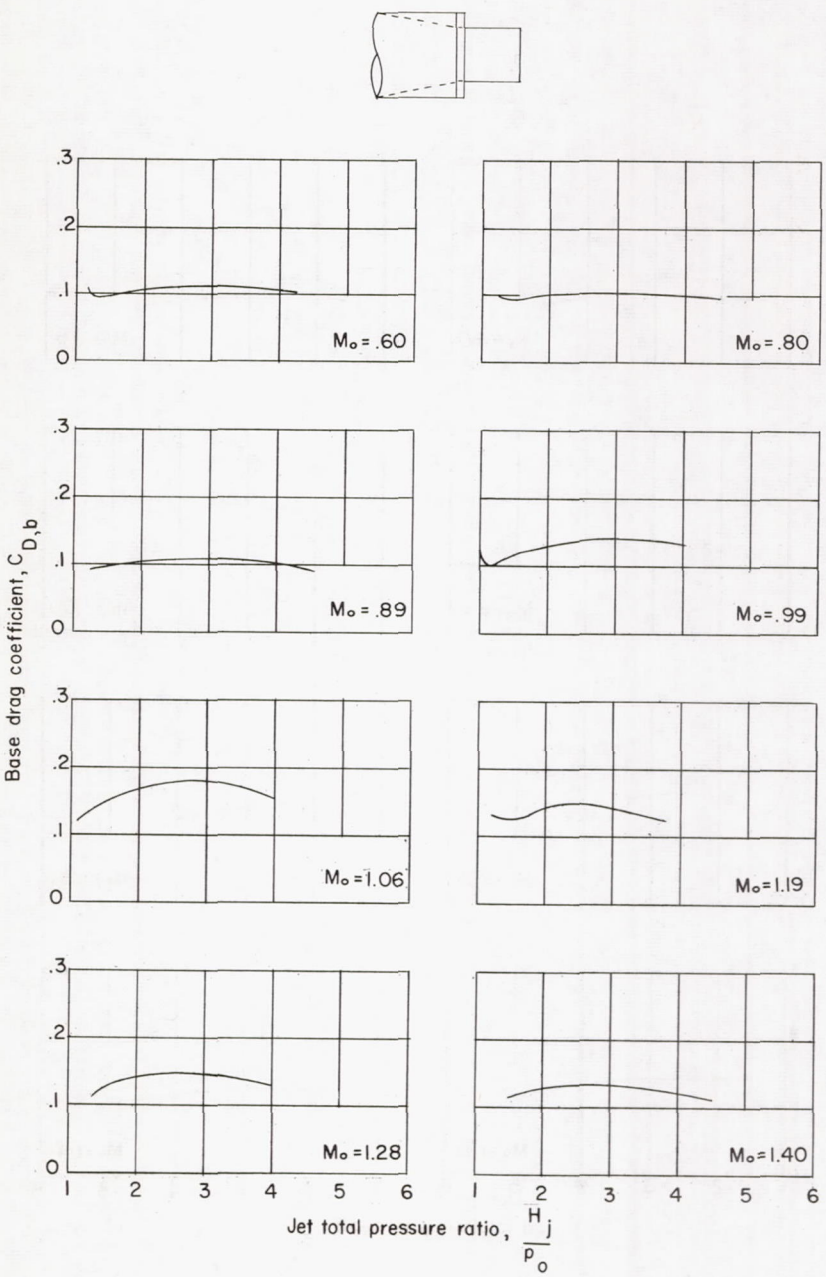
(a) Nozzle extended 0 inch.

Figure 4.- Effect of jet on base drag of single jet configuration with sonic nozzles.



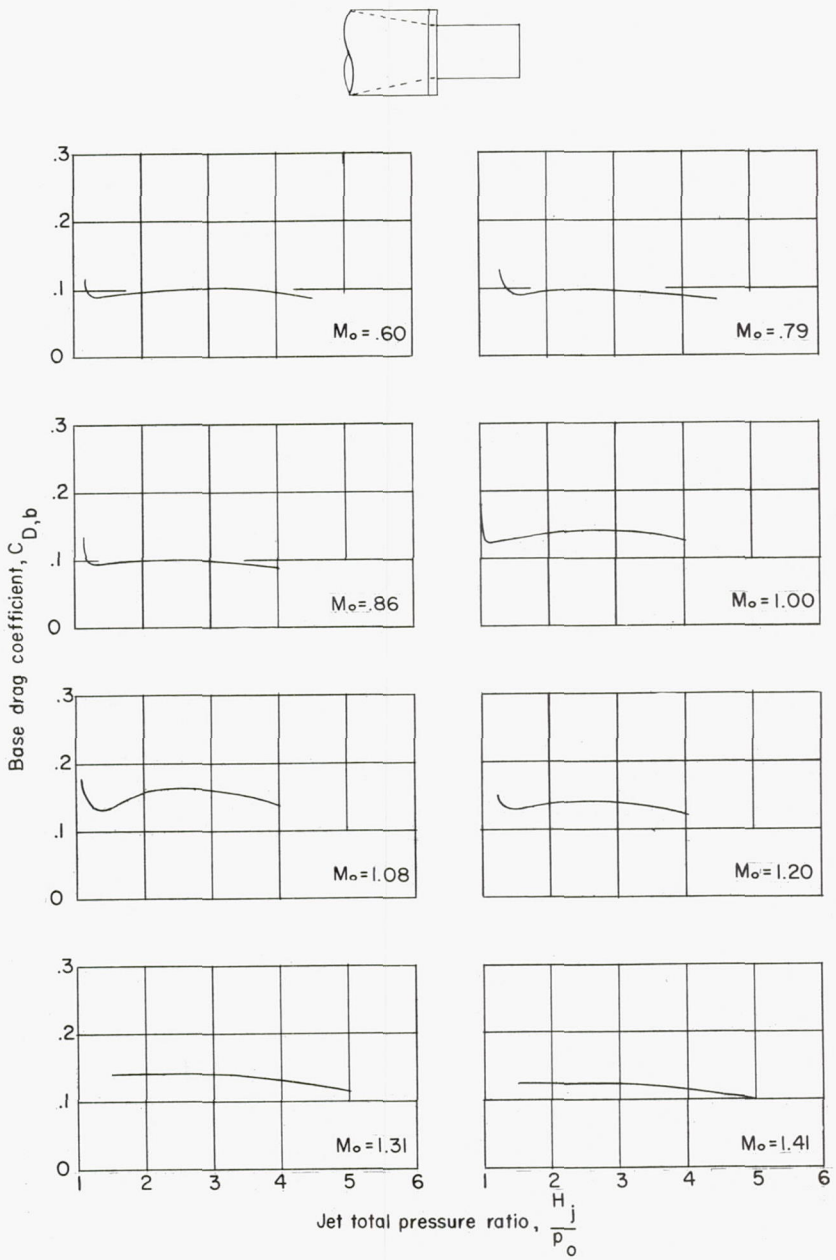
(b) Length of nozzle extension, 0.315 inch.

Figure 4.- Continued.



(c) Length of nozzle extension, 0.625 inch.

Figure 4.- Continued.



(d) Length of nozzle extension, 0.960 inch.

Figure 4.- Concluded.

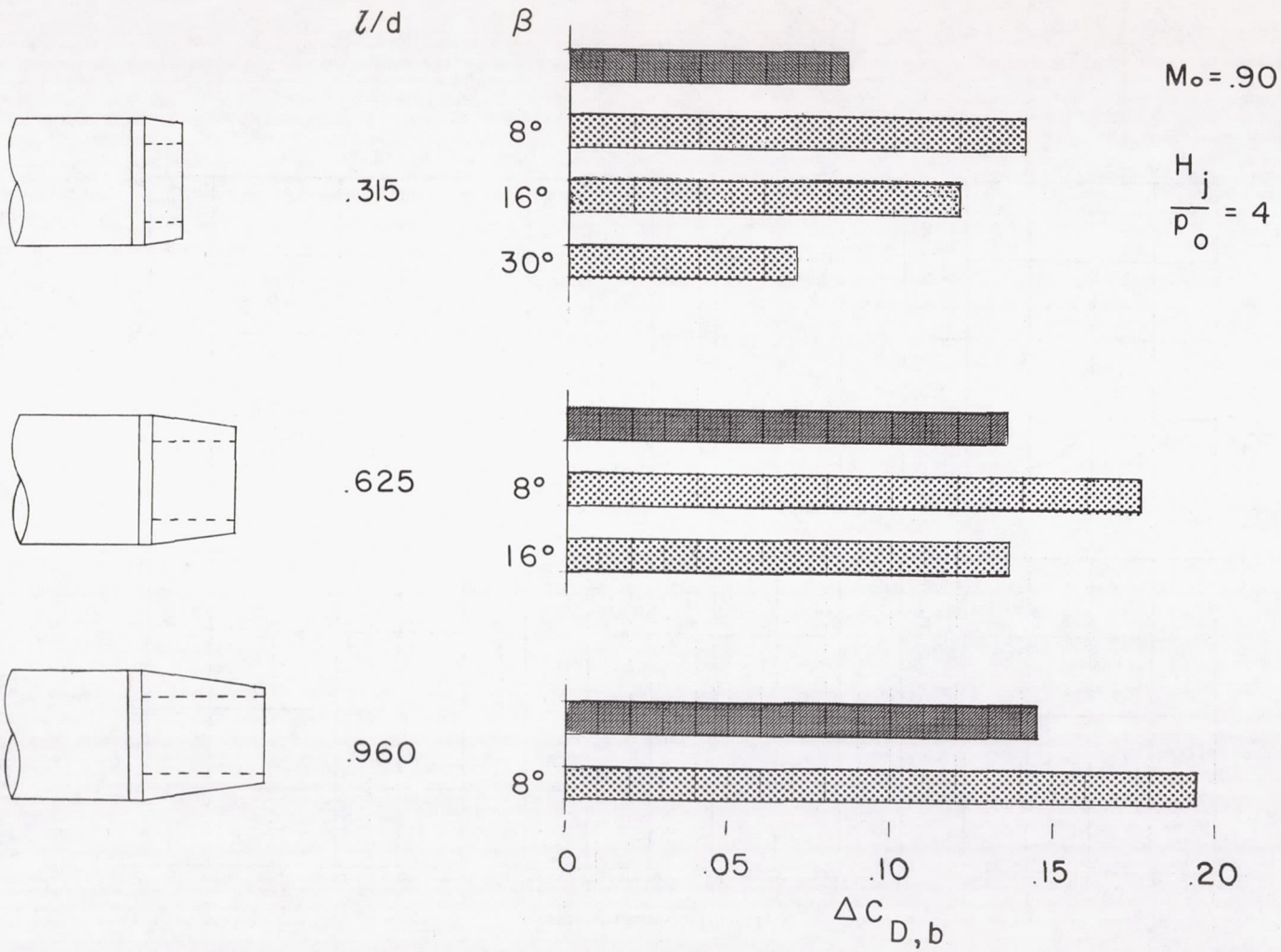
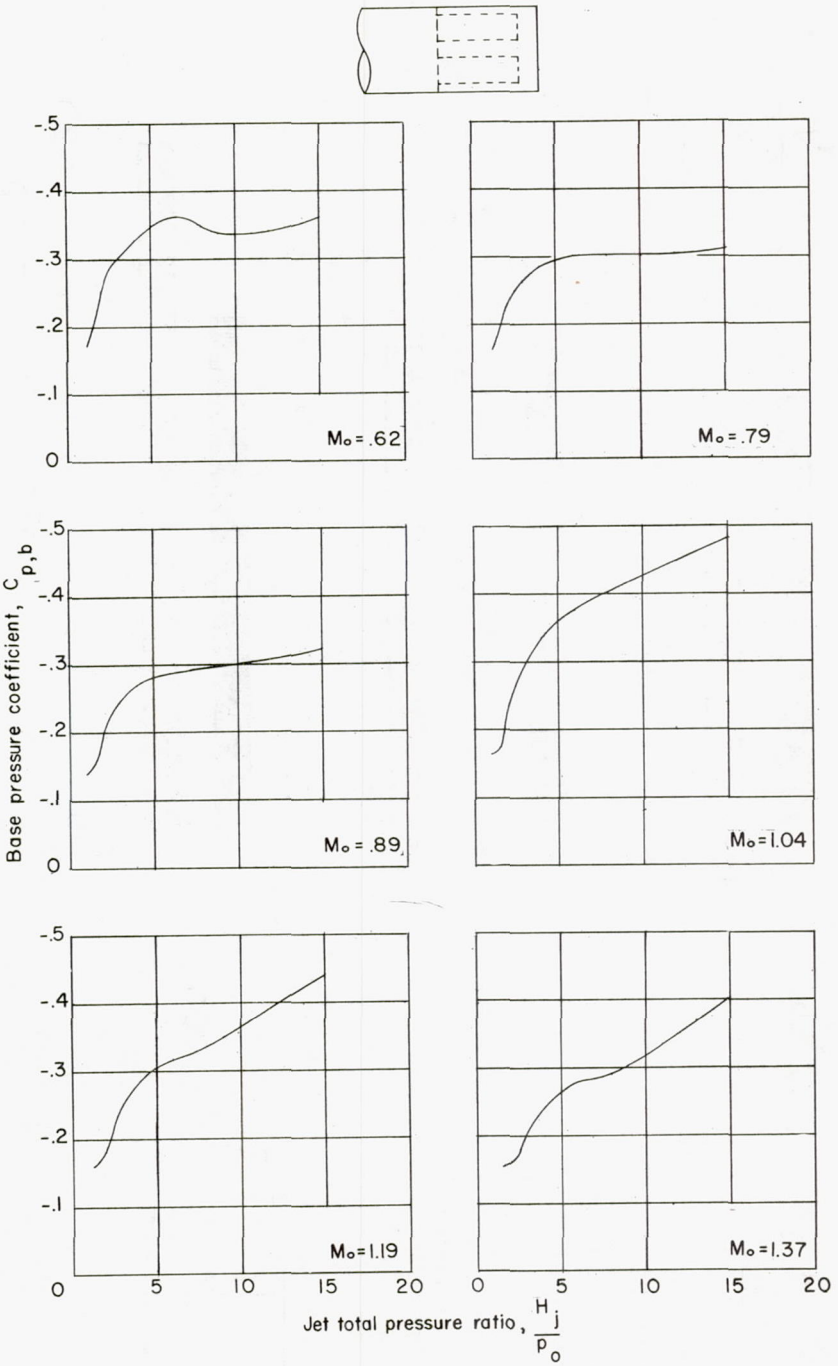
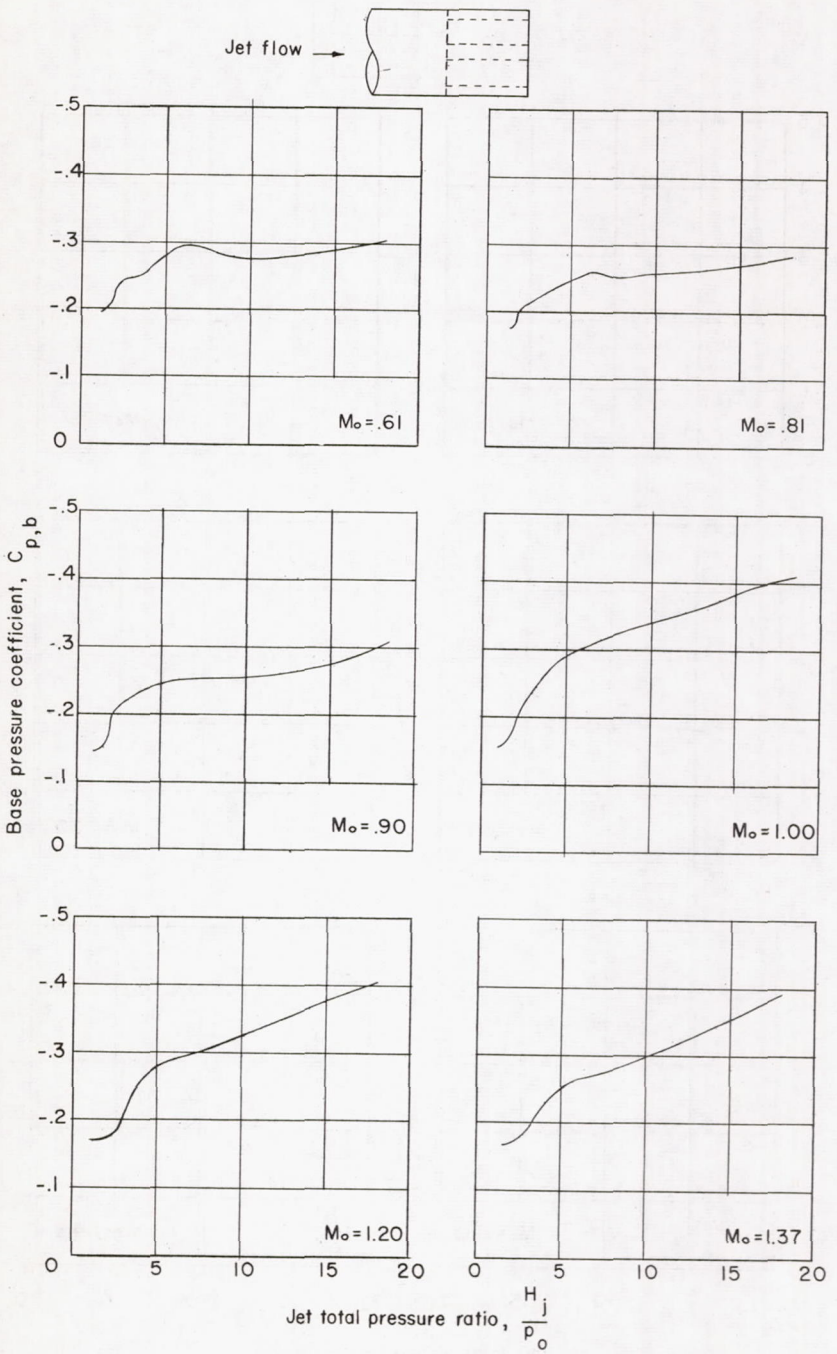


Figure 5.- Single-jet drag summary of extended nozzles compared with boattailed bodies. The incremental drag coefficient $\Delta C_{D,b}$ is below that of a cylindrical model with jet in the plane of base.



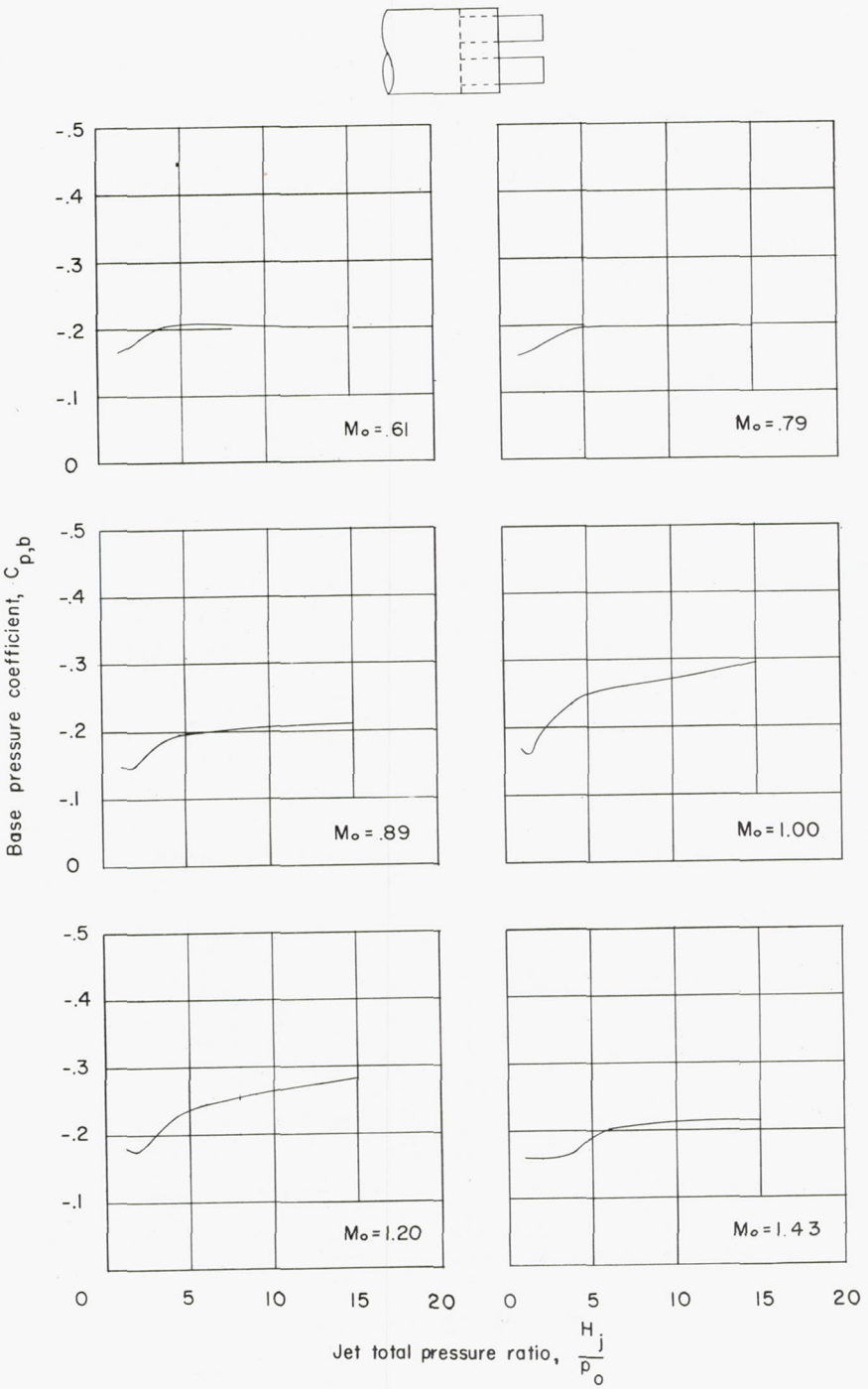
(a) Length of nozzle extension, -0.210 inch.

Figure 6.- Effect of jet on base drag of twin-jet configuration with supersonic nozzles.



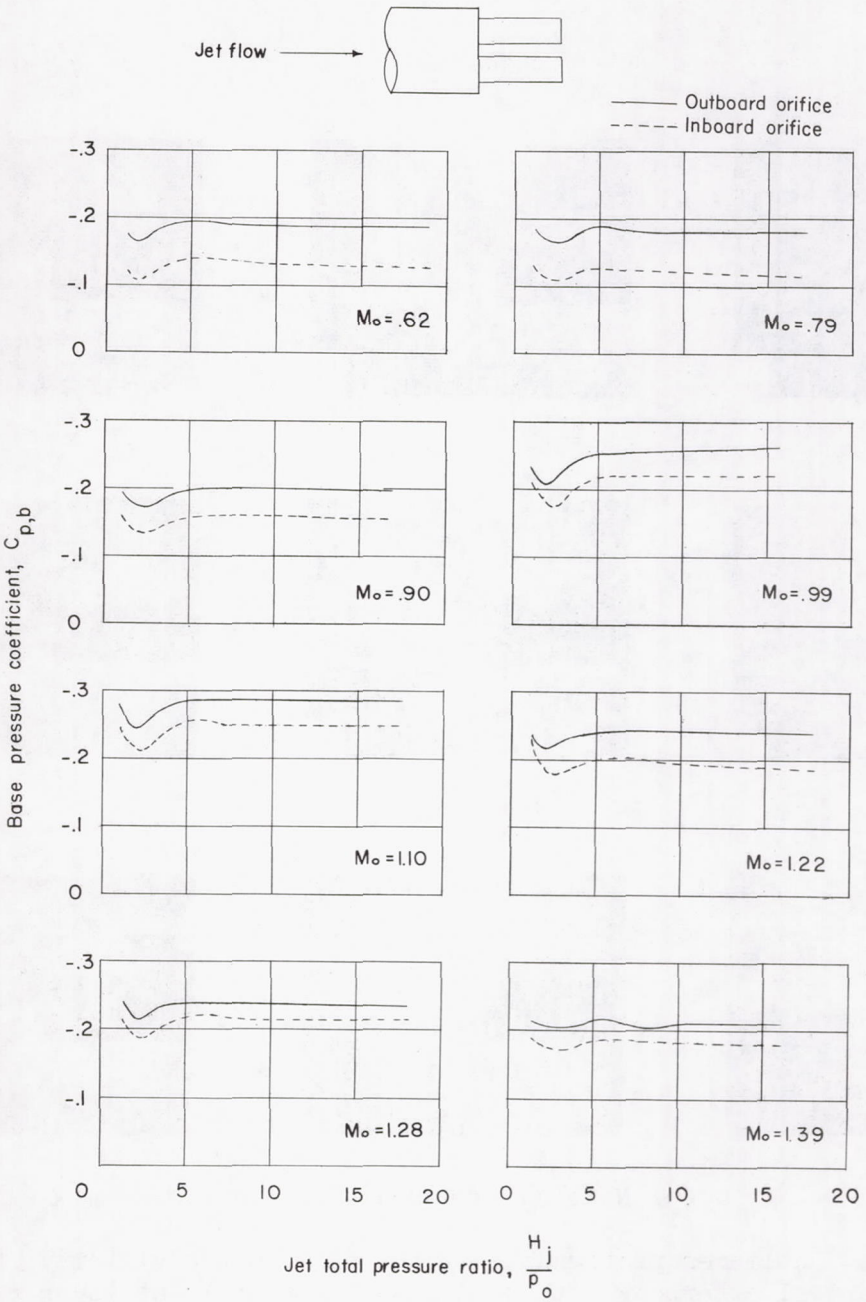
(b) Length of nozzle extension, 0.020 inch.

Figure 6.- Continued.



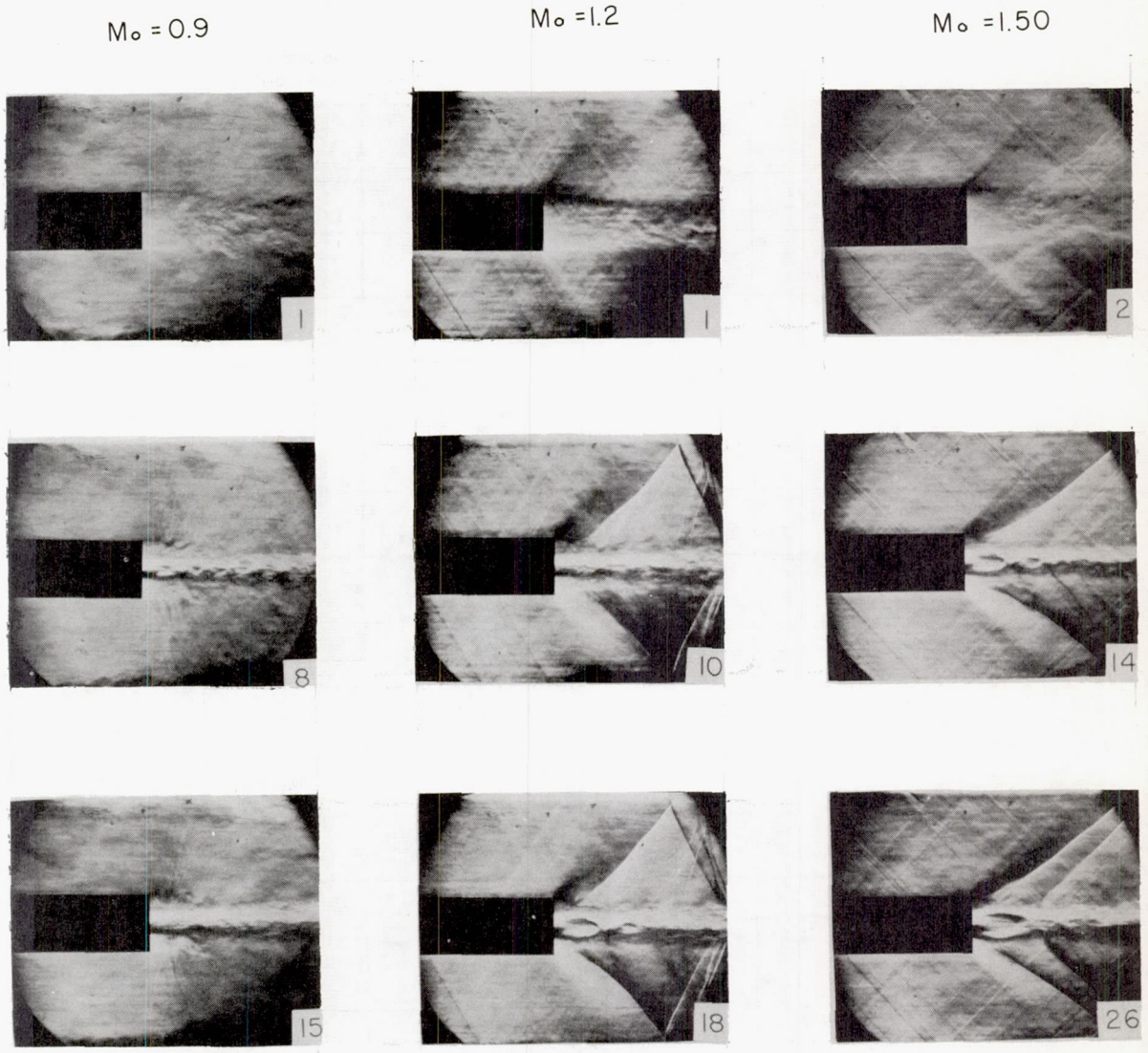
(c) Length of nozzle extension, 0.480 inch.

Figure 6.- Continued.



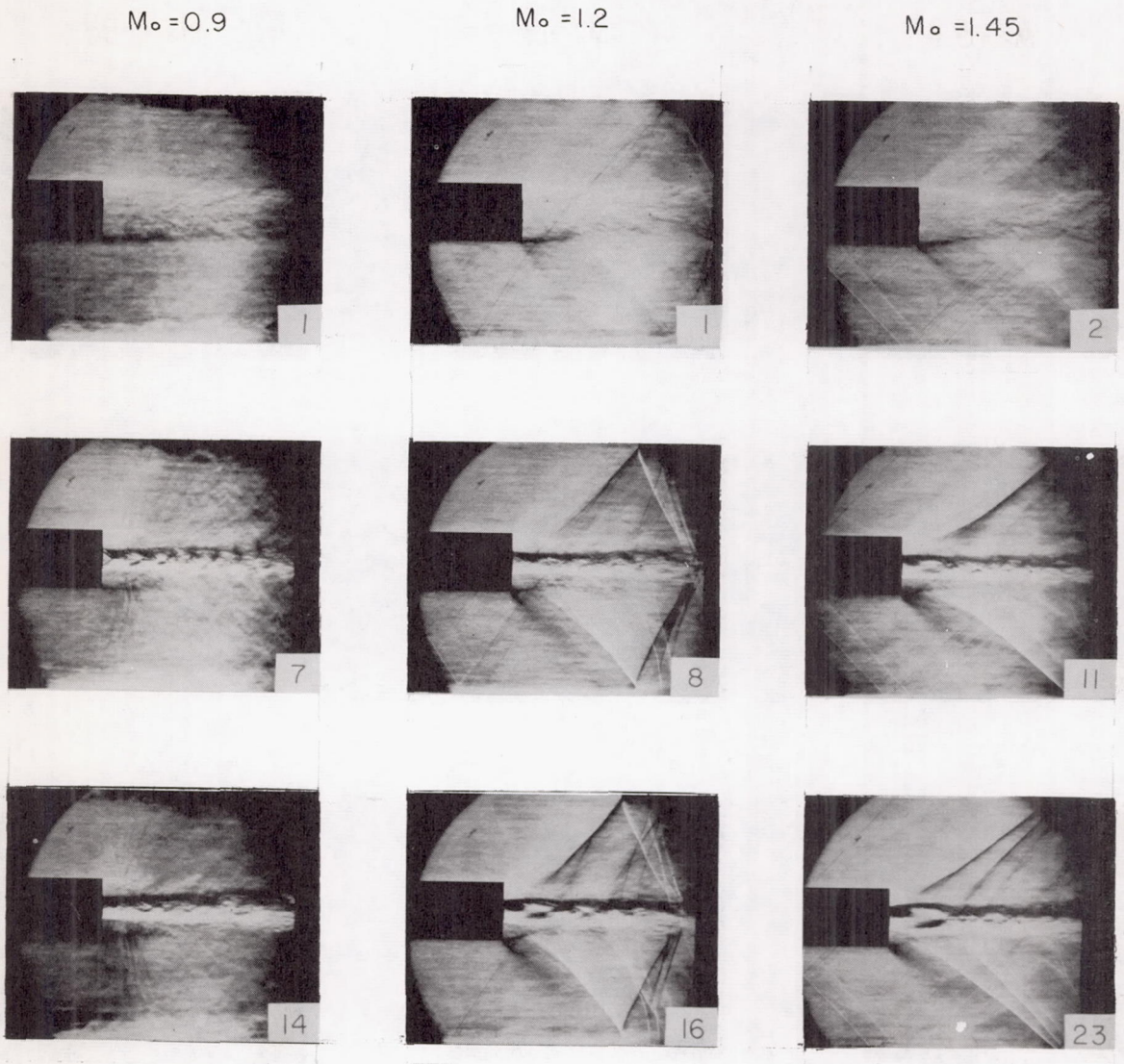
(d) Length of nozzle extension, 0.960 inch.

Figure 6.- Concluded.



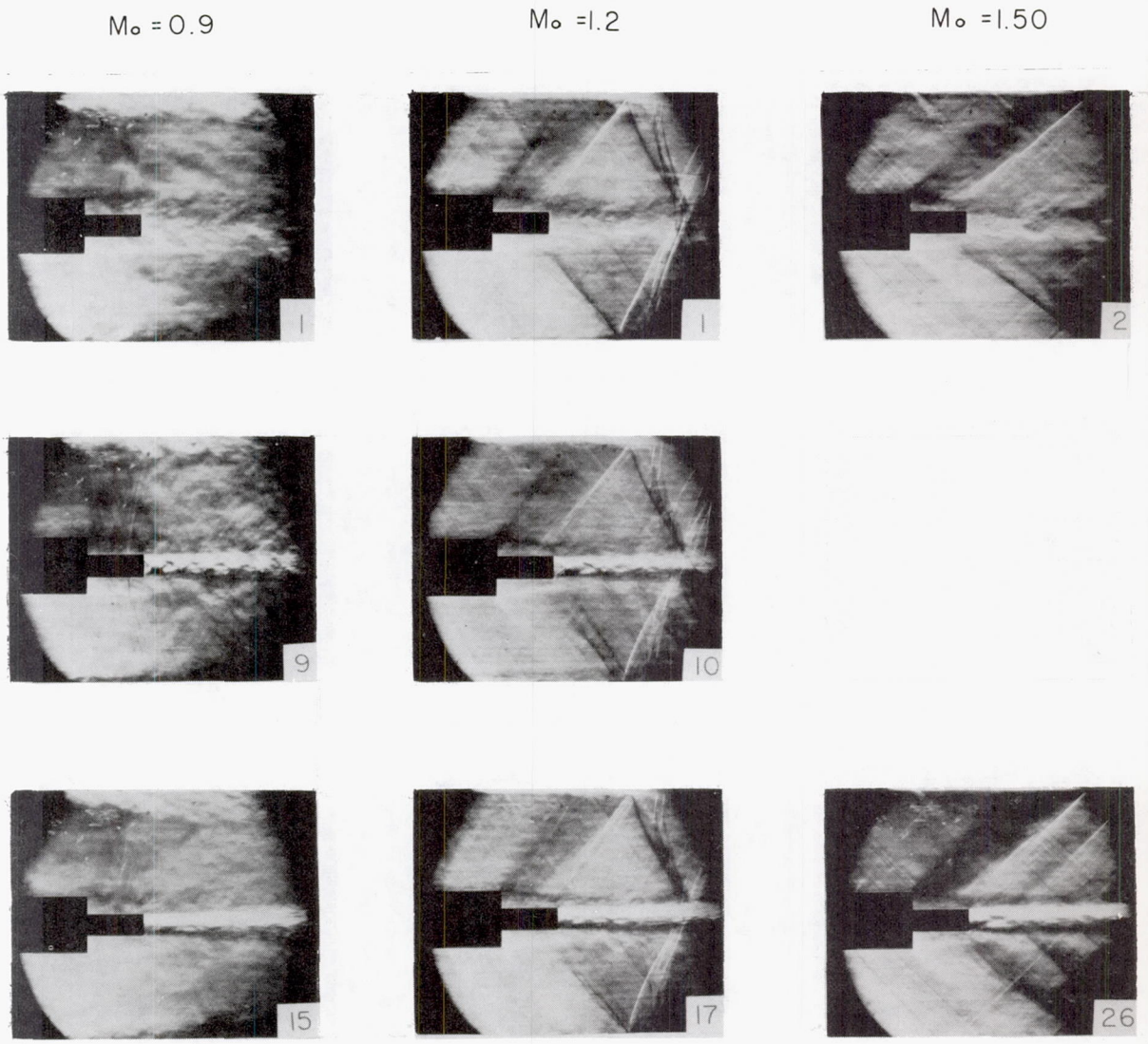
(a) Nozzles extended -0.21 inch. L-58-105

Figure 7.- Schlieren photographs of the flow in the vicinity of the cylindrical afterbody with twin-jets. (Numerals at lower right corner of each figure indicate jet total pressure ratio.)



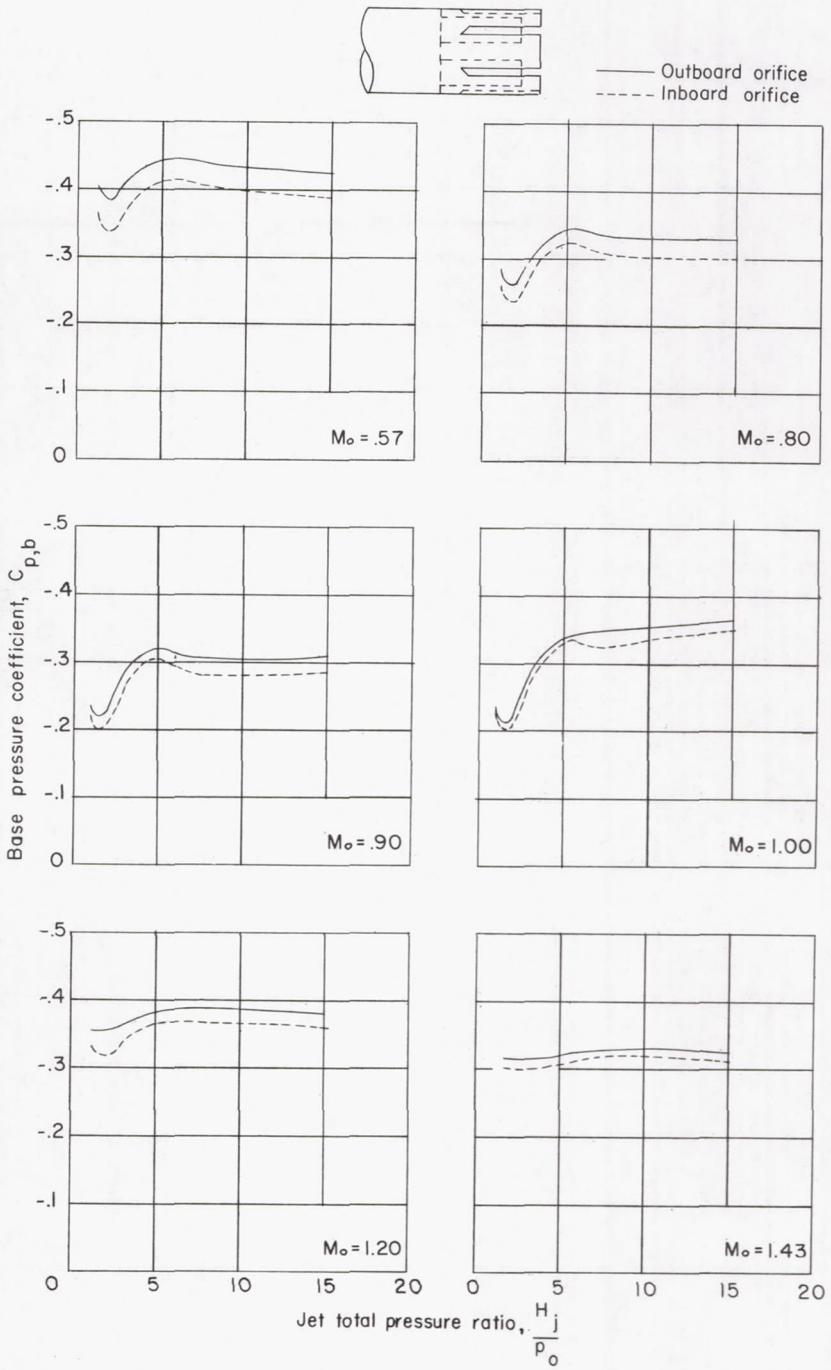
(b) Nozzles extended 0.02 inch. L-58-106

Figure 7.- Continued.



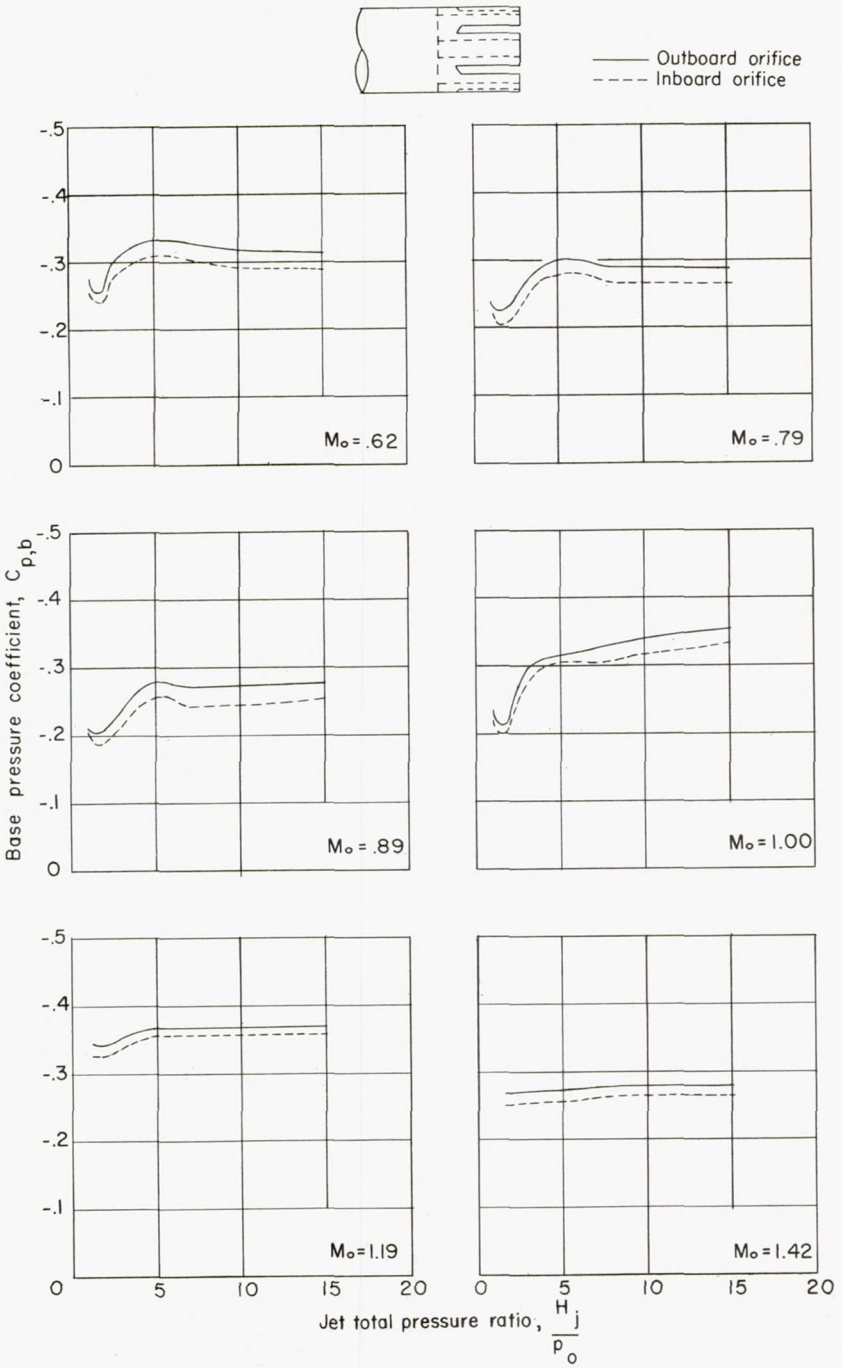
(c) Nozzles extended 0.960 inch. L-58-107

Figure 7.- Concluded.



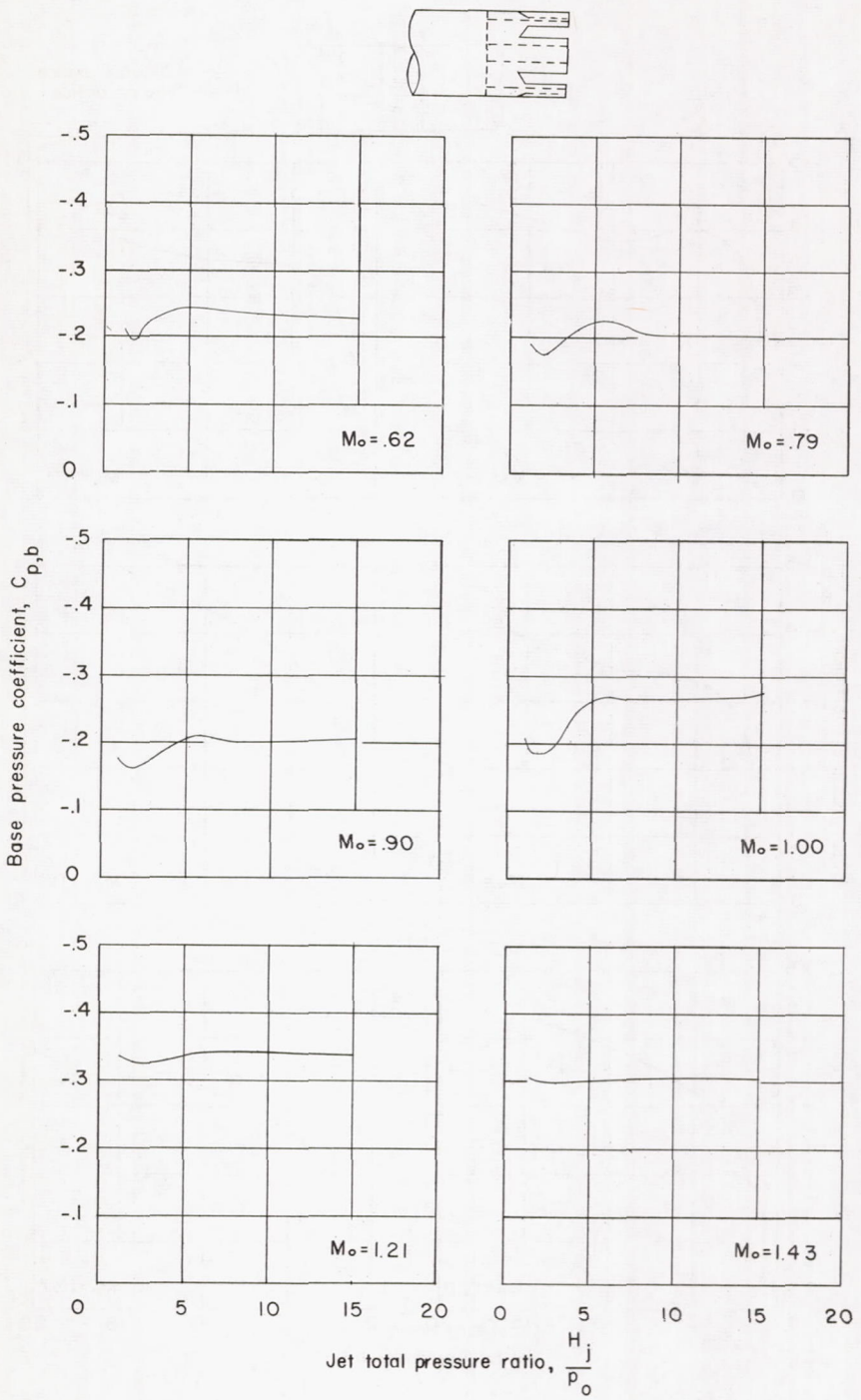
(a) l = -0.21; 6 longitudinal slots; sleeve 26 percent open.

Figure 8.- Jet effects on drag of twin-jet configuration with ventilated base cavity.



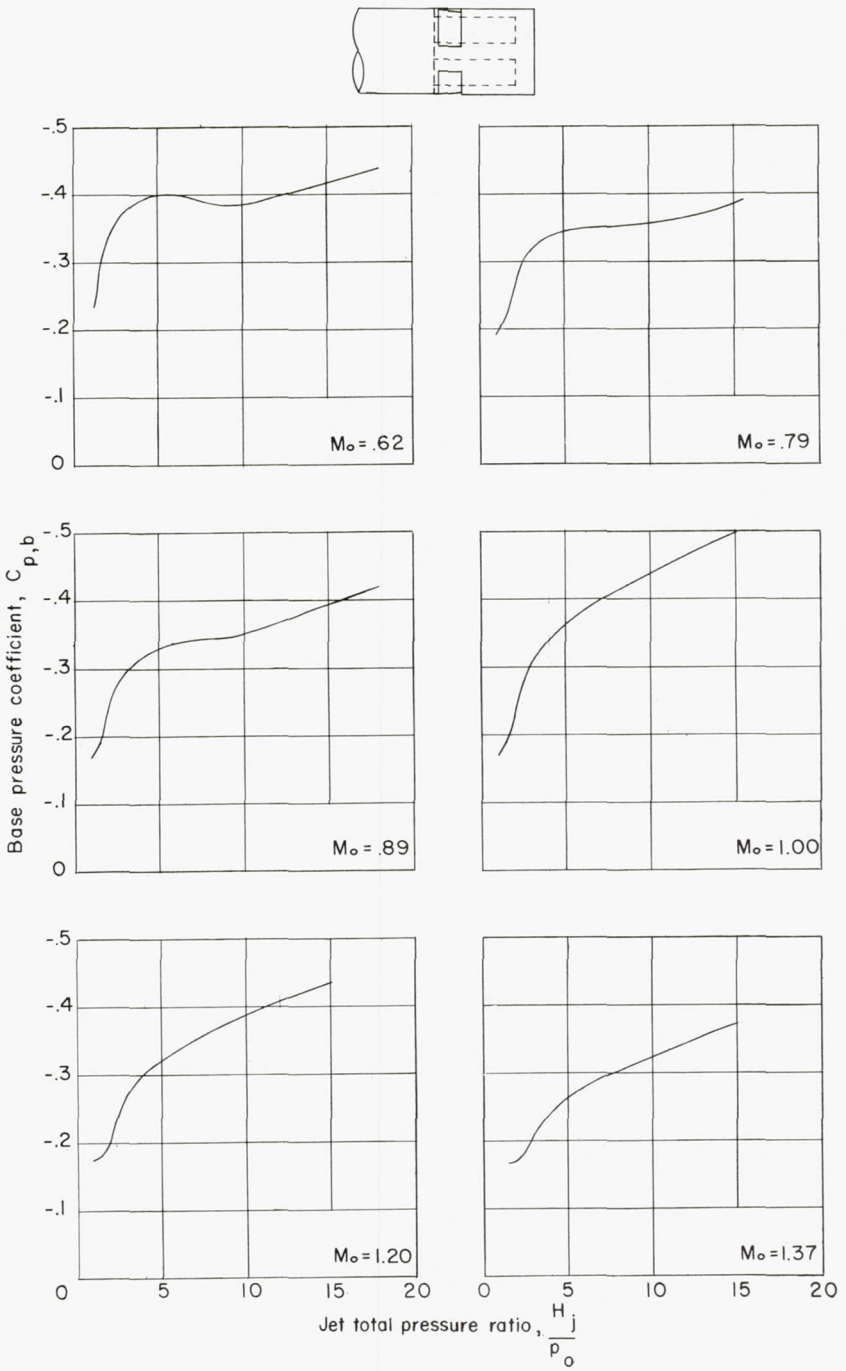
(b) l = 0.02; 6 longitudinal slots; sleeve 26 percent open.

Figure 8.- Continued.



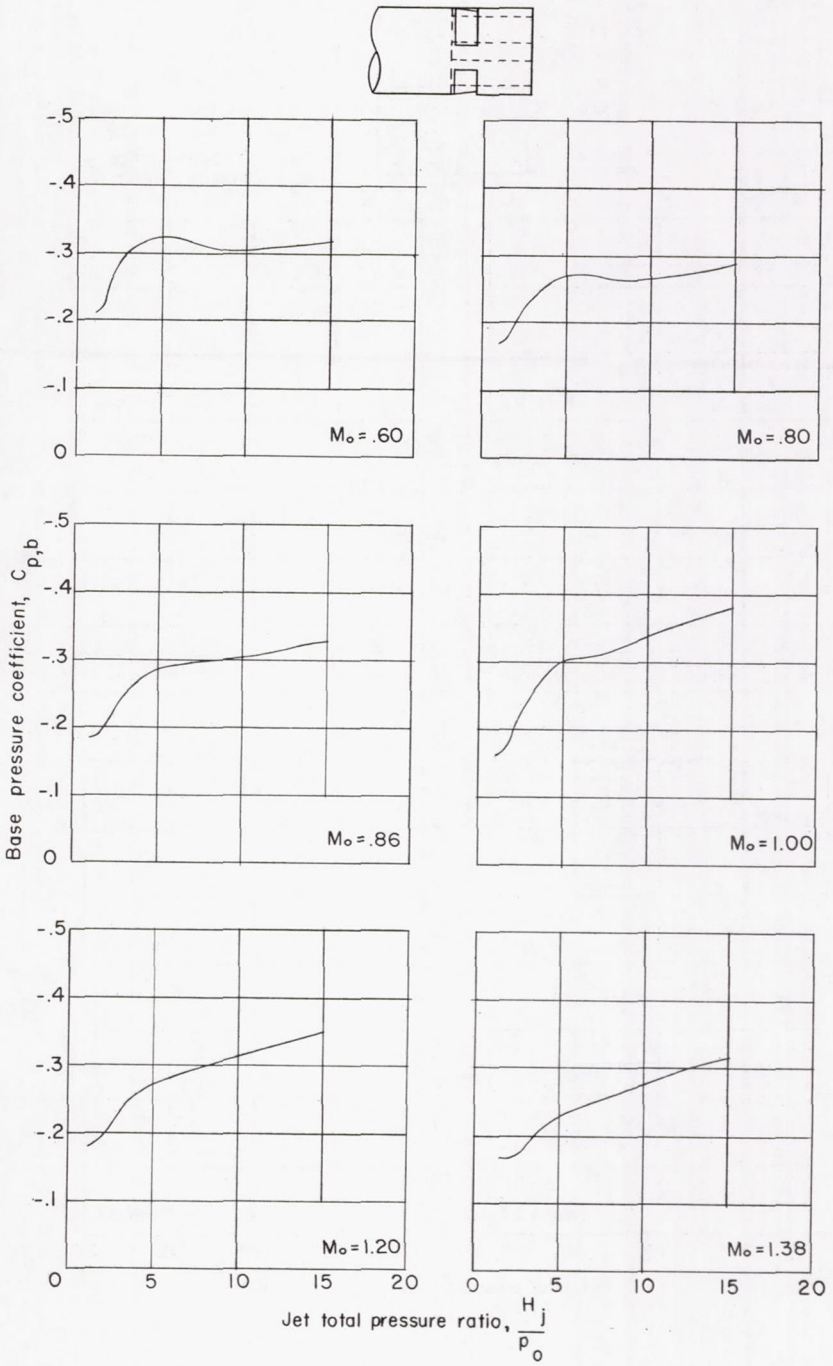
(c) ℓ = 0.02; 6 longitudinal slots; sleeve 52 percent open.

Figure 8.- Continued.



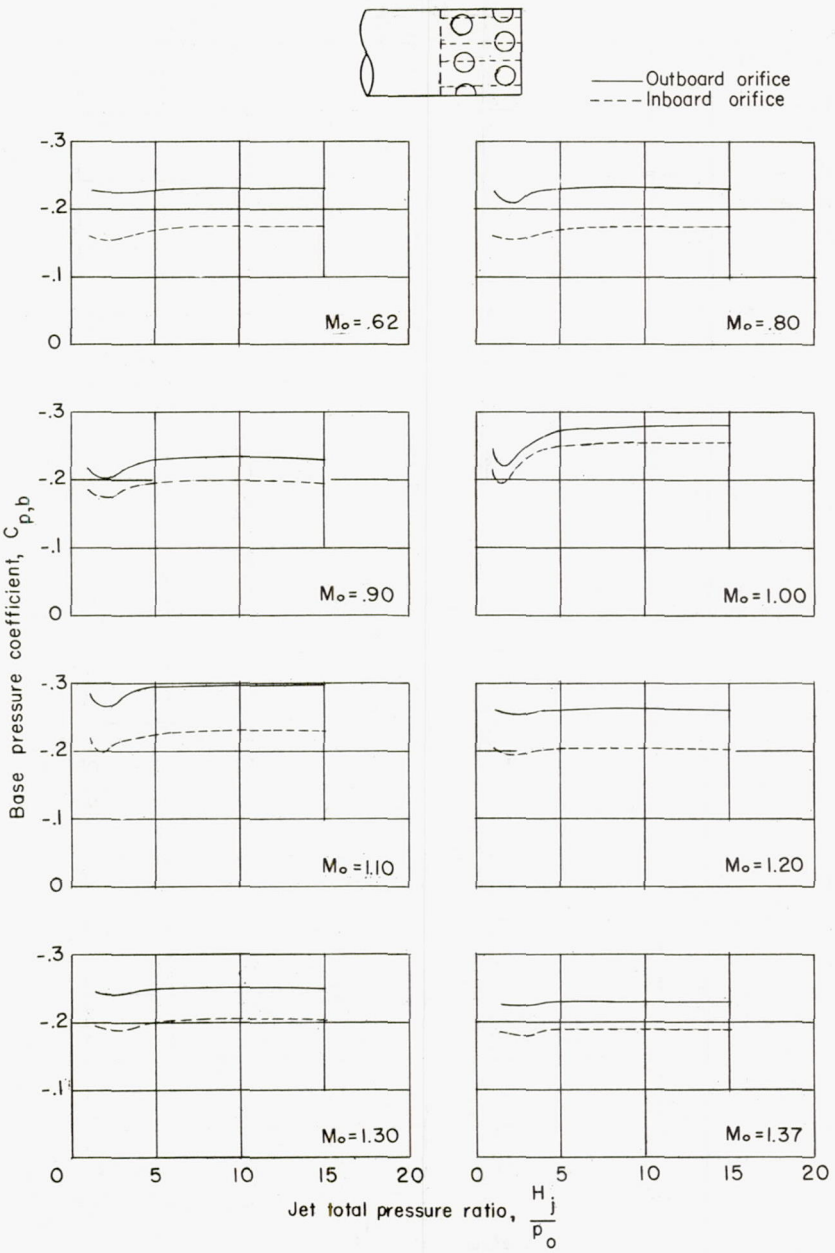
(d) l = -0.21; circumferential slot.

Figure 8.- Continued.



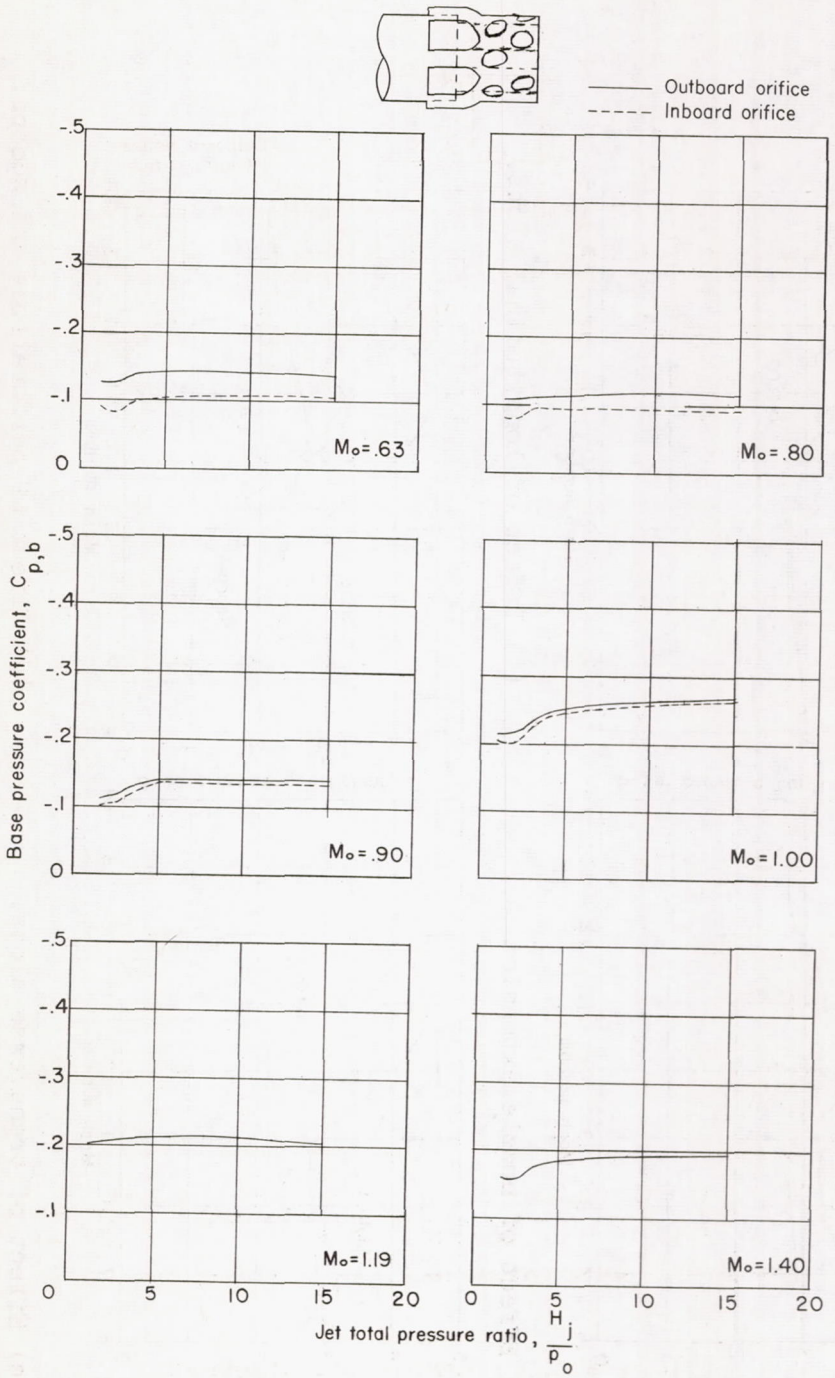
(e) ℓ = 0.02; circumferential slot.

Figure 8.- Continued.



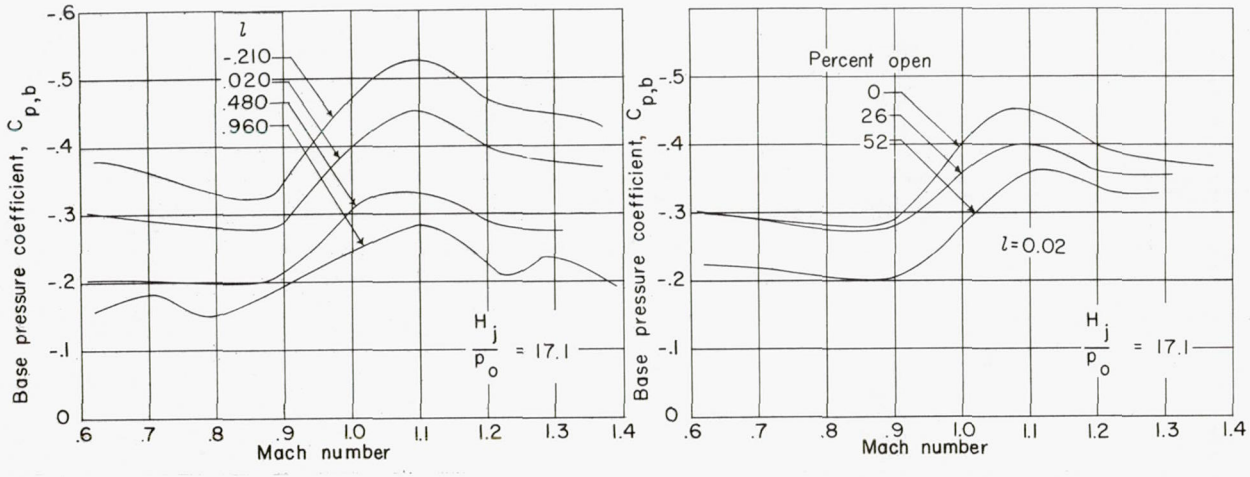
(f) λ = 0.02; perforated sleeve.

Figure 8.- Continued.



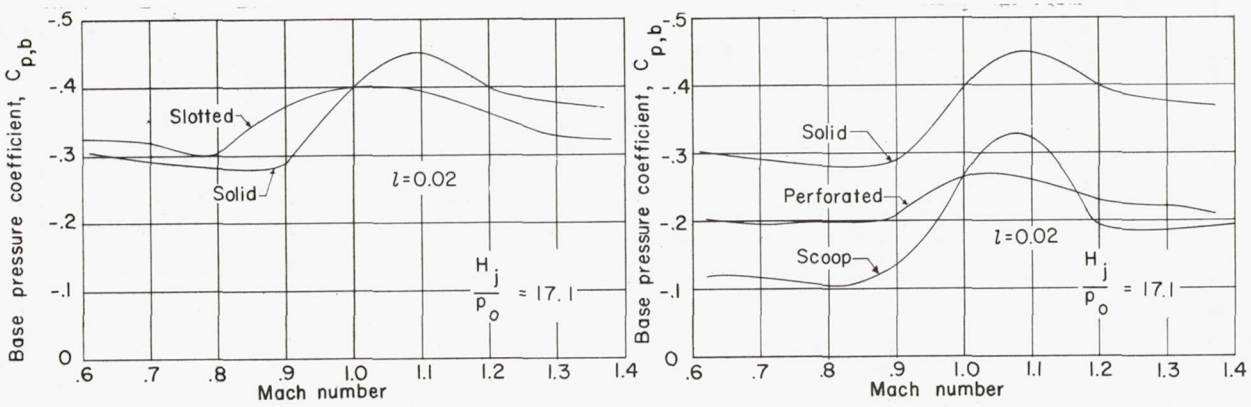
(g) l = 0.02; perforated sleeve with scoops.

Figure 8.- Concluded.



(a) Effect of nozzle extension.

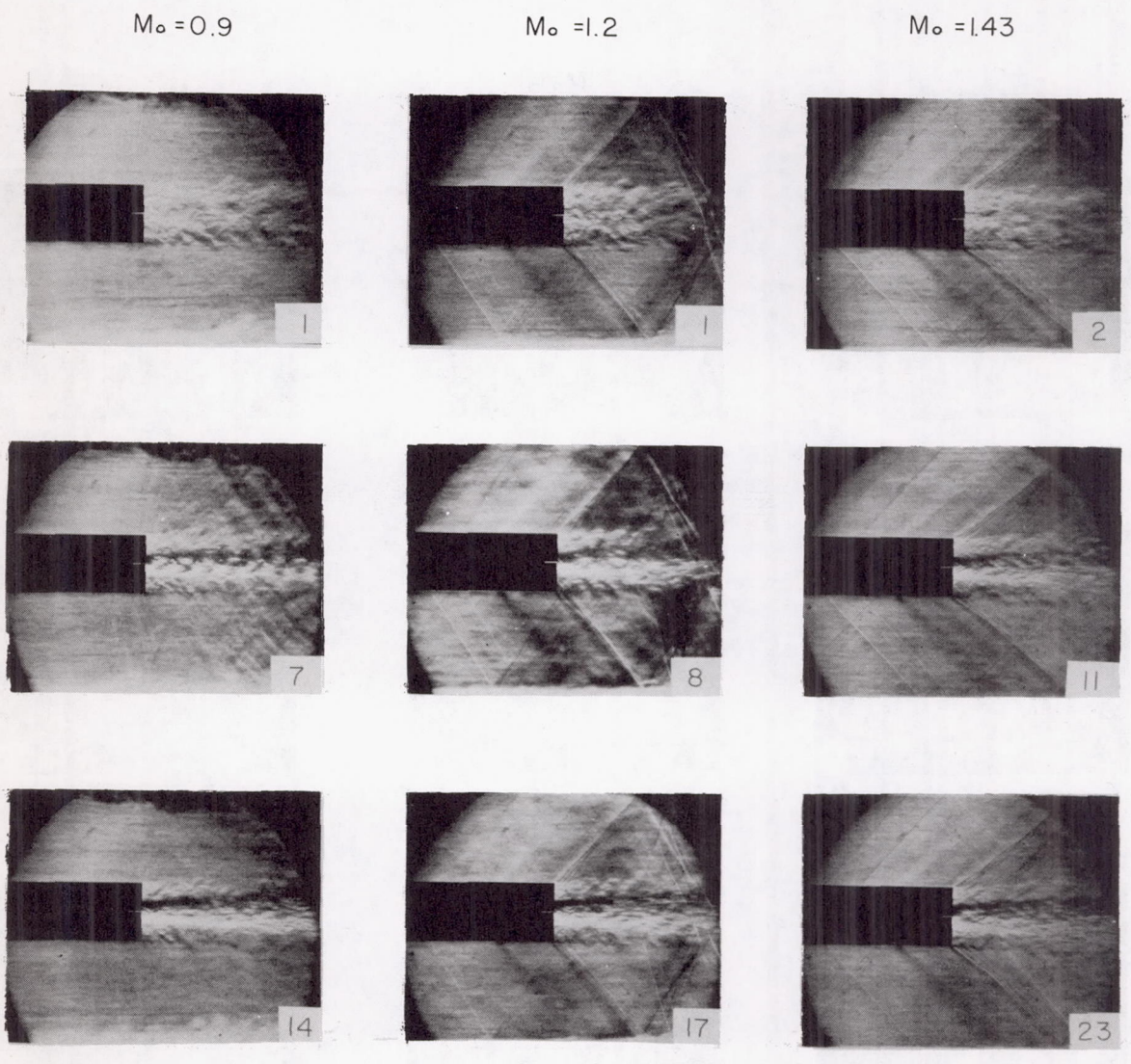
(b) Effect of longitudinal slots.



(c) Effect of transverse slots.

(d) Effect of perforations and scoops.

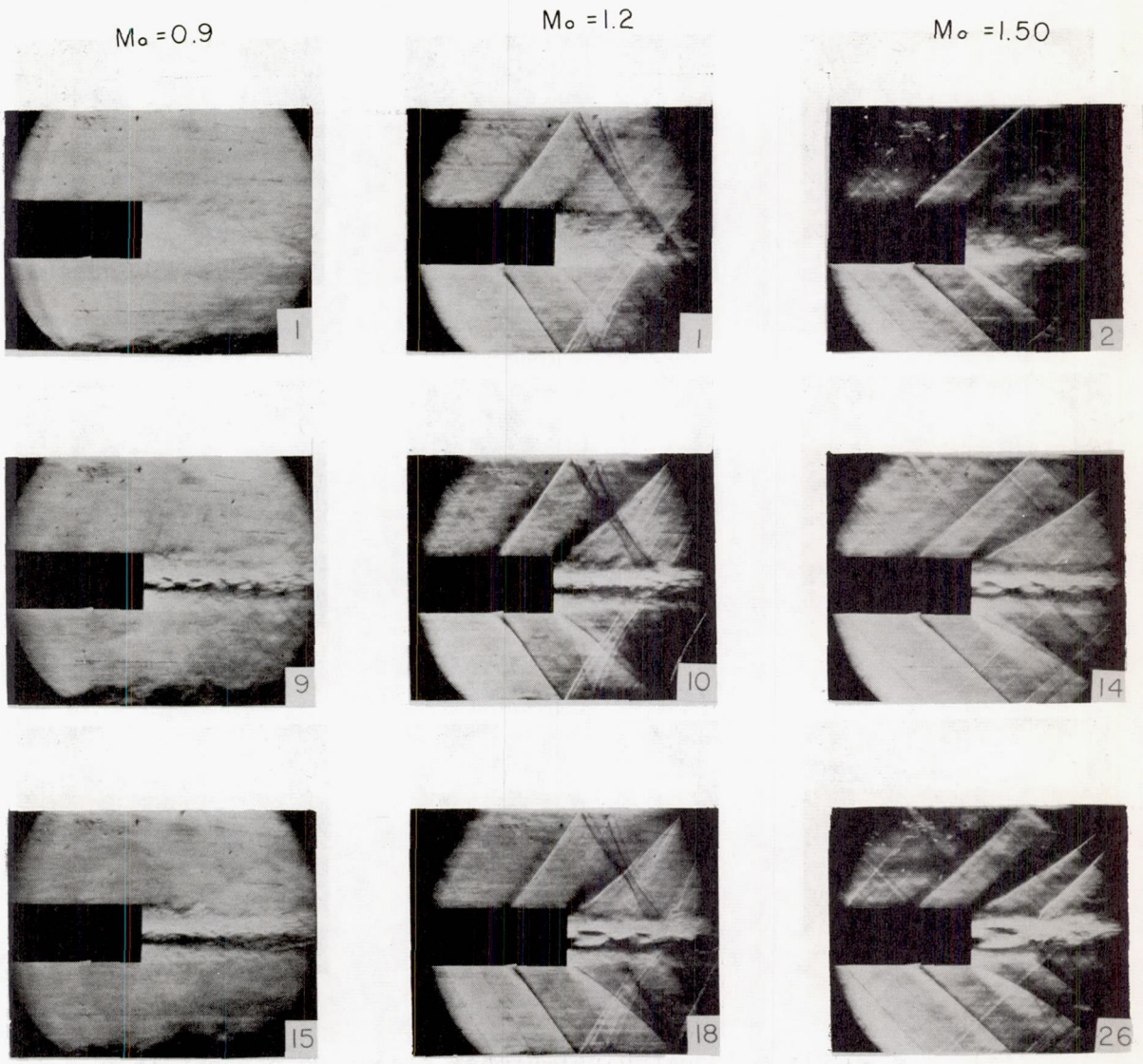
Figure 9.- Effect of nozzle extension and base ventilation on base pressure for twin-jet configurations at design pressure ratio. H_j/p_o = 17.1.



L-58-108

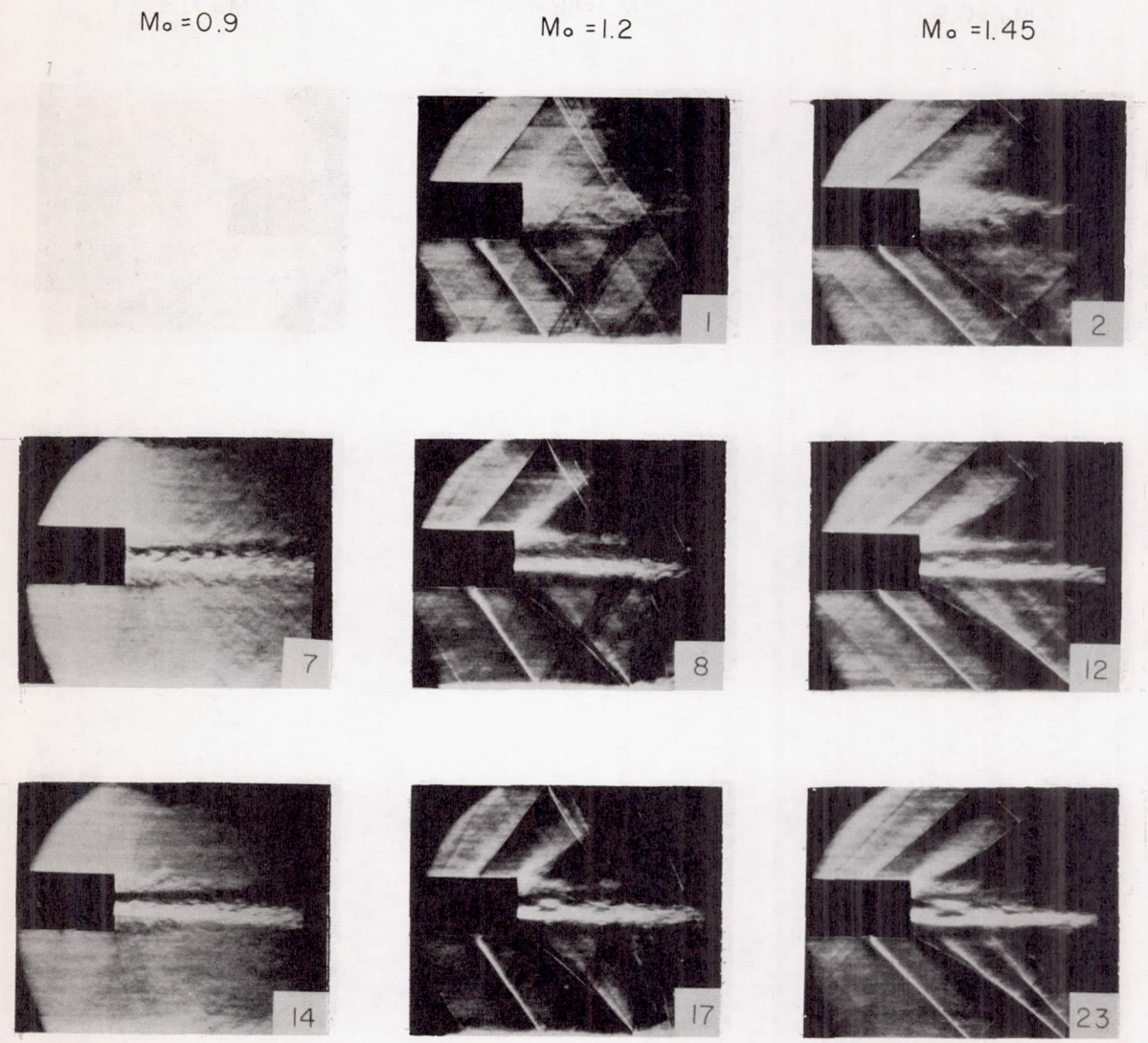
(a) λ = -0.21; 6 longitudinal slots; sleeve 26 percent open.

Figure 10.- Schlieren photographs of the flow in the vicinity of the base bleed afterbody with twin jets. (Numerals at lower right corner of each figure indicate jet total-pressure ratio.)



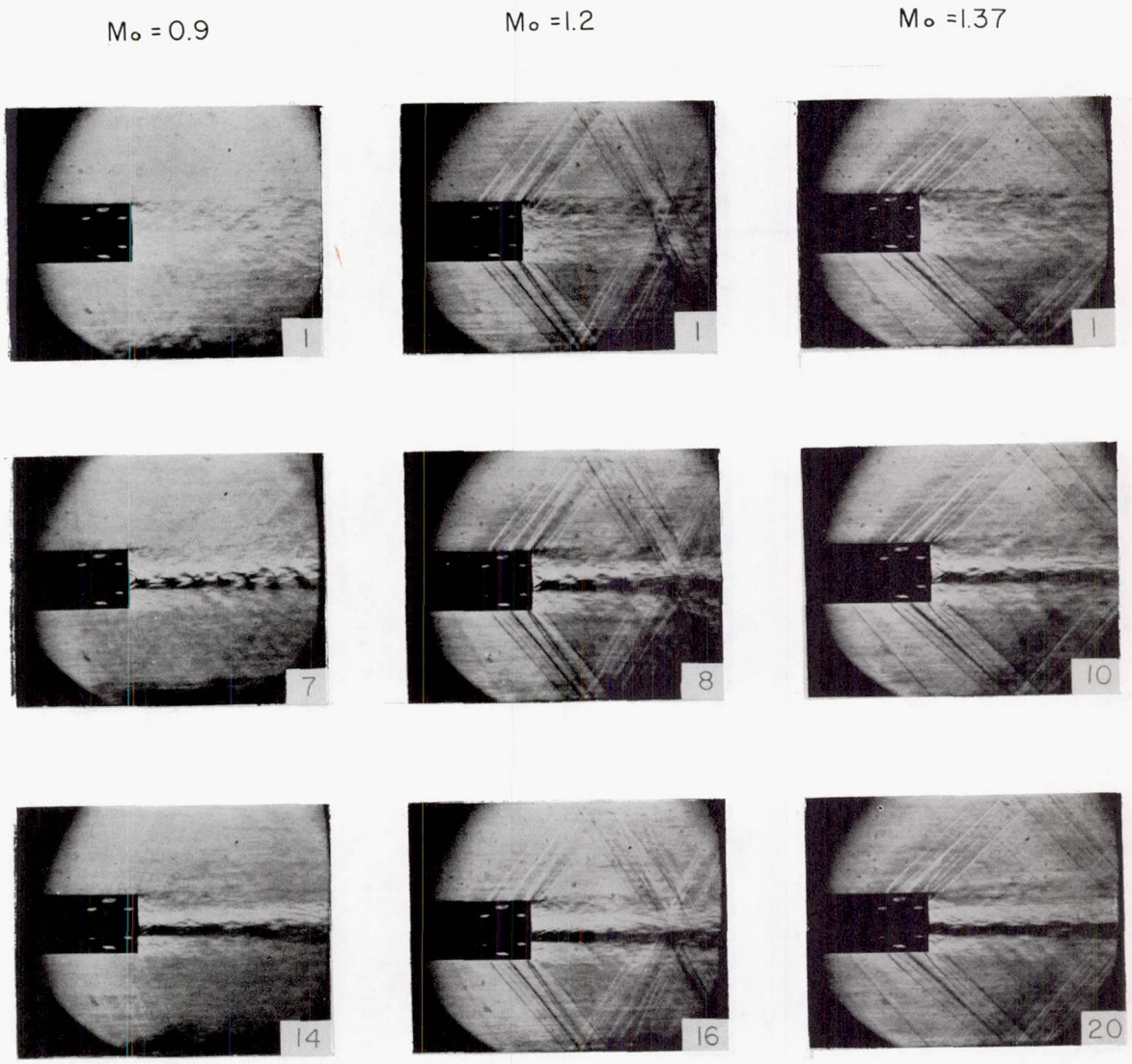
(b) ℓ = -0.21; circumferential slot. L-58-109

Figure 10.- Continued.



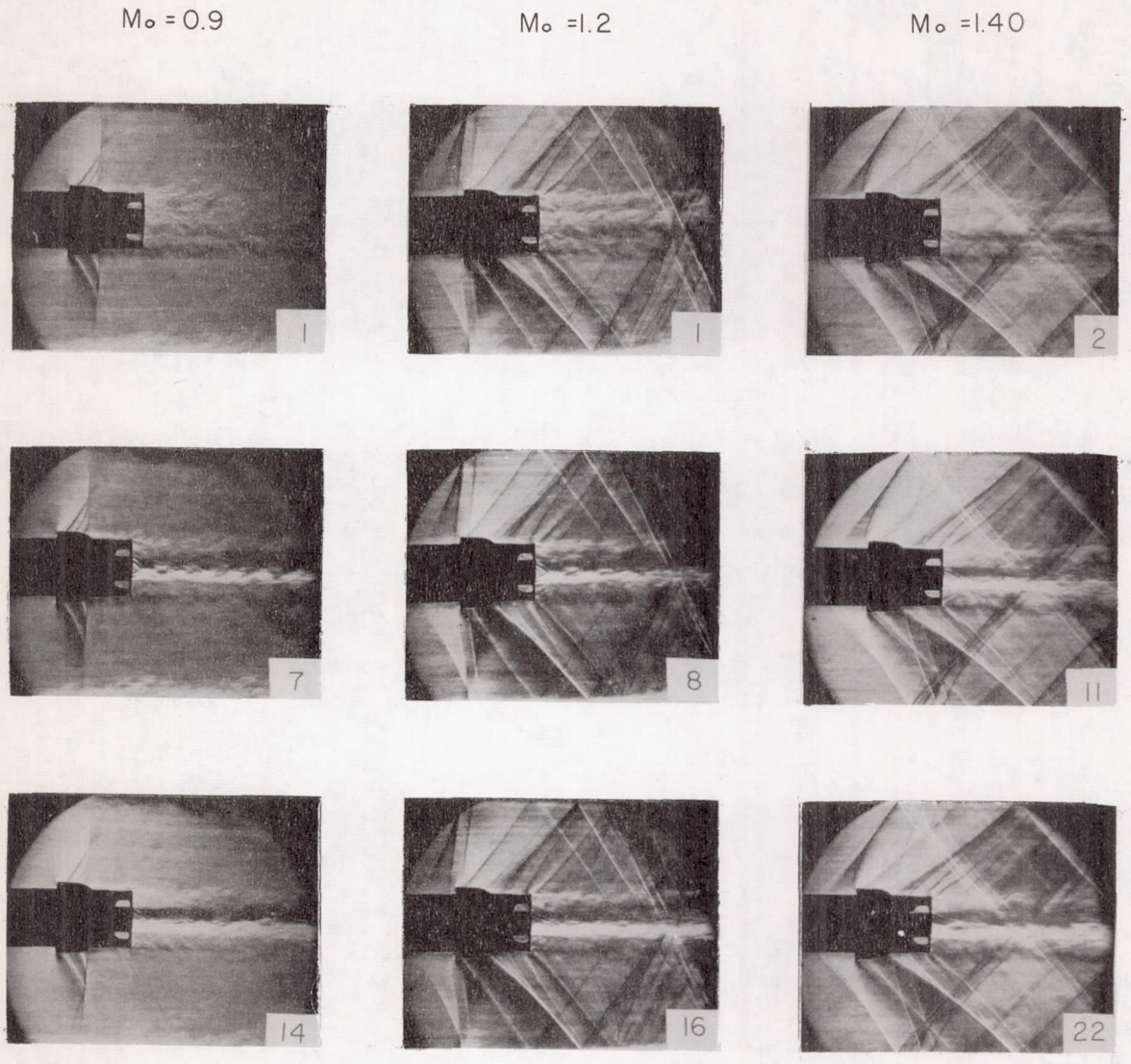
(c) ℓ = 0.02; circumferential slot. L-58-110

Figure 10.- Continued.



(d) l = 0.02; perforated sleeve. L-58-111

Figure 10.- Continued.



(e) l = 0.02; perforated sleeve with scoops. L-58-112

Figure 10.- Concluded.